

**Efficiency of copper oxide nanoparticle
combined with ultrafiltration membrane for
treatment of hexavalent chromium
contaminated sewage water**

**A thesis submitted in partial fulfillment of the requirements
for the award of degree of**

Master of Technology in Material Engineering

Jadavpur University

2023

by

Gourav Chatterjee

Examination Roll No.: M4MAT23003

Registration No.: 160308 of 2021-2022

Under the guidance and supervision of

Dr. Sathi Banerjee

**DEPARTMENT OF METALLURGICAL AND MATERIAL
ENGINEERING
JADAVPUR UNIVERSITY
KOLKATA – 700032, WEST BENGAL**

Dedicated
To my beloved parents

**Whose love, support and sacrifice motivated me to complete this work
within stipulated time**

Certificate

This is to certify that the thesis entitled, “**Efficiency of copper oxide nanoparticle combined with ultrafiltration membrane for treatment of hexavalent chromium contaminated sewage water**” submitted by **Mr. Gourav Chatterjee (Examination Roll No: M4MAT23003 and Registration No: 160308 of 2021-2022)** in partial fulfillment of the requirements for the award of the degree of **Master of Technology in Material Engineering** from **Jadavpur University, Kolkata** is an authentic work carried out by him under my guidance and supervision.

To the best of my knowledge, the information contained in this thesis has not been submitted to any other University/ Institute for the award of any degree or diploma.

Prof. Pravash Chandra Chakraborti

Head
Department of Metallurgical and
Material Engineering
Jadavpur University
Kolkata - 700032

Dr. Sathi Banerjee

Associate Professor
Department of Metallurgical and
Material Engineering
Jadavpur University
Kolkata - 700032

Prof. Ardhendu Ghoshal

Dean
Faculty of Engineering and Technology
Jadavpur University
Kolkata - 700032

Declaration of Originality and Compliance of Academic Ethics

I hereby declare that this thesis **“Efficiency of copper oxide nanoparticle combined with ultrafiltration membrane for treatment of hexavalent chromium contaminated sewage water”** contains literature survey and original research work by the undersigned candidate, as a part of my M.Tech Degree in Material Engineering during academic session 2021-2023. All the information that has been provided in this document is in accordance with academic rules and ethical conduct. I also declare that, as required by this rules and conduct, I have fully cited and referred all materials and results that are not original to this work.

Name: Gourav Chatterjee

Examination Roll Number: M4MAT23003

Registration Number: 160308 of 2021-2022

Place: Kolkata

Date:

Signature

Certificate of Approval

The foregoing thesis is hereby approved as a credible study of an engineering subject and presented in a manner satisfactory to warrant acceptance as pre-requisite to the degree for which it has been submitted. It is understood that by this approval the undersigned do not necessarily endorse or approve any statement made, opinion expressed or conclusion drawn there in but approve the thesis only for which it is submitted.

Examiners for the final evaluation of the thesis:

Date:

Signature of the Examiners

Place: Kolkata

Acknowledgement

While completing this M.Tech final year project, I have come across a number of people whose contributions helped me in various ways in successful completion of my thesis work and they deserved special thanks. It's my pleasure to express my gratitude to all of them.

I would like to take this opportunity to express my sincere gratitude to my project guide **Dr. Sathi Banerjee, Associate Professor, Department of Metallurgical and Material Engineering, Jadavpur University** for providing the necessary guidance that was required to complete the research work within the stipulated amount of time. I am deeply obliged for her motivation, immense knowledge and assistance during the course of the research work. I feel extremely lucky for having a kind hearted guide and mentor like her.

I am deeply indebted to **Prof. Pravash Chandra Chakraborti**, Head of the Department, Metallurgical and Material Department, Jadavpur University, whose immense guidance helped me throughout the period of my project work.

It gives me immense pleasure and happiness in acknowledging the help and support of **Dr. Priyankari Bhattacharya**, WOS – B(DST), Department of Metallurgical and Material Engineering, Jadavpur University. Without her guidance, this research work would have been completed with utmost perfection. I am also thankful for her immense support in writing this thesis.

I am deeply indebted to my family members for their moral support and continuous encouragement while carrying out this study. I want to thank all my classmates for providing accompany and support throughout the year.

I am also thankful to Mr. Partha Sarathi Das, Lab Assistant, Department of Metallurgical and Material Engineering, Jadavpur University, for providing technical help during the experimental work in Materials Lab.

I would be thankful to the almighty god for keeping me healthy and in good faith throughout the course of this research work.

Name: Gourav Chatterjee

Place: Kolkata

Contents

Certificate	ii
Declaration of Originality and Compliance of Academic Ethics	iii
Certificate of Approval	iv
Acknowledgement	v
Contents	vi
List of Figures	viii
List of Tables	viii
Abstract	ix
Chapter 1. Introduction	1
1.1. Nanotechnology in Waste Water Treatment	1
1.2. Synthesis of Nanoparticles	2
1.3. Green Synthesis of Nanoparticles	3
1.4. Biological Components of Green Synthesis	4
1.5. Green synthesis copper oxide nanoparticles by plant extracts	4
Chapter 2. Literature Review	6
Chapter 3. Materials and methods	11
3.1. Materials and Equipment Used	11
3.1.1. List of Apparatus	11
3.1.2. List of Chemicals	11
3.1.3. Plant Used	11
3.2. Methodology	12
3.2.1. Green Synthesis of CuO NPs	12
3.2.1.1. Preparation of Precursors	12
3.2.1.2. Synthesis of Nanoparticles	13
3.2.2. Chromium removal study	15
3.2.2.1. Application of CuO NPs in Chromium removal	15
3.2.2.2. Preparation of dichromate solution	15
3.2.2.3. Equilibrium Study	15
3.2.2.4. Kinetic Study	16
Chapter 4. Characterization of Materials	17
4.1. FTIR spectroscopy	17

4.2. XRD.....	19
4.3. FESEM & EDS.....	21
4.4. Ultrafiltration (UF) Membrane Study.....	23
4.4.1. Procedure	23
4.4.2. Specification	23
4.4.3. Wastewater characterization	24
4.5. Seed Germination Study	25
4.5.1. Procedure	25
Chapter 5. Results and Discussion	26
Characterization of CuO NPs	26
5.1. FTIR.....	26
5.2. XRD.....	29
5.3. FESEM and EDS	31
5.4. Removal study of Cr (VI) using CuO NPs	34
5.4.1. Effect of adsorbent dose.....	34
5.4.2. Effect of Contact time	35
5.4.3. Effect of initial concentration of Dichromate Solution.....	36
5.4.4. Effect of pH.....	37
5.5. Ultrafiltration Membrane study	38
5.5.1. Flux versus Time Study	38
5.5.2. Flux versus Transmembrane Pressure Study	39
5.6. Effect of chromium on mustard seed germination	40
5.6.1. Effect of different un-treated and treated solutions on seed germination.....	40
5.6.2. Toxicity on Root and Shoot Elongation.....	42
Chapter 6. Conclusion	43
Chapter 7. Future Scope	44
References	45

List of Figures

Figure 1: Different synthesis process of nanoparticles	3
Figure 2: Different steps involved in synthesis of CuO nanoparticles	5
Figure 3: Membrane filtration Pump Setup.....	11
Figure 4: Jackfruit tree (<i>Artocarpus heterophyllus</i>)	11
Figure 5: Schematic diagram of different steps involved in synthesis of copper oxide nanoparticles.....	14
Figure 6: Green synthesized CuO NPs (before and after adsorption of chromium)	16
Figure 7: Kinetic Study Experiment.....	16
Figure 8: IR Prestige-21 FTIR measuring instrument.....	18
Figure 9: SmartLab SE XRD measuring instrument.....	20
Figure 10: FESEM and EDS measuring instrument	22
Figure 11: FTIR of CuO NPs (Before biosorption)	28
Figure 12: FTIR of CuO NPs (After biosorption).....	28
Figure 13: Crystal Structure of CuO NPs.....	29
Figure 14: XRD of green synthesized CuO NPs	30
Figure 15: FESEM images of CuO NPs (Before biosorption).....	31
Figure 16: EDS of CuO NPs (Before biosorption)	32
Figure 17: FESEM images of CuO NPs (After biosorption)	32
Figure 18: EDS of CuO NPs (After biosorption).....	33
Figure 19: Adsorbent dose versus removal	34
Figure 20: Contact time versus removal	35
Figure 21: Initial chromium concentration versus removal	36
Figure 22: pH value versus removal	37
Figure 23: Graph showing Flux versus Time study	38
Figure 24: Graph showing Flux versus Transmembrane pressure study	39
Figure 25: Study of seed germination (24 Hrs).....	40
Figure 26: Study of seed germination (48 Hrs).....	40
Figure 27: Study of seed germination (72 Hrs).....	41
Figure 28: Percent seeds germinated w.r.t days	41
Figure 29: RLST w.r.t days	42

List of Tables

Table 1: FTIR functional groups	27
Table 2: Crystalline Size from XRD data	30
Table 3: Waste water characterization (before and after membrane study).....	39

Abstract

Copper Oxide Nanoparticles were green synthesized using leaf extracts of *Artocarpus heterophyllus*. The synthesized nanoparticles were washed, dried and kept for further use. Samples were characterized in terms of X-Ray Diffraction (XRD), Fourier Transform Infrared Spectroscopy (FTIR), Field Emission Scanning Electron Microscope (FESEM), Energy Dispersive X-Ray Spectroscopy (EDS) etc. Average crystallite size of nano powders was calculated from full width at half maxima of XRD Peaks. Debye-Scherrer formula was used for the calculation of crystallite size which was found to be 16.092 nm. Average lattice parameter was found to be 4.411 Å. Spherical morphology of the NPs was confirmed from FESEM micrographs. Potassium dichromate solution was used for observing heavy metal removal efficiency by synthesized CuO NPs. For a fixed nanoparticle dose of 10 g/L and initial chromium concentration of 30ppm, removal of chromium increased with increase in contact time. Removal efficiency of 61.54% and 80.05% was obtained at 60 mins of contact time at pH 2 for green synthesized nano particles.

Keywords: Nanoparticles, Copper Oxide, Green synthesis, FTIR, XRD, FESEM, EDS, Adsorption, Chromium removal.

Chapter 1. Introduction

Due to the growth of industry and human activities like electroplating industry, batteries, pesticides, mining industry, rayon industry, metal rinse processes, tanning industry, fluidized bed bioreactors, textile industry, metal smelting, petrochemicals, paper manufacturing, and electrolysis applications, there is a sharp increase in presence of heavy metals in wastewater day by day. [1] The threatening of the environment, human health and the ecosystem is on its peak as waste water contaminated with heavy metal is finding its way into ecosystem. [2] The heavy metals are severely dangerous because they are non-biodegradable and carcinogenic. That is why there can be critical health issues due to the presence of heavy metals in water.

Small amount of heavy metals like lead (Pb), zinc (Zn), mercury (Hg), nickel (Ni), cadmium (Cd), copper (Cu), chromium (Cr), and arsenic (As) are present in waste water but they are still hazardous to human health and environment. Metals like silver (Ag), iron (Fe), manganese (Mn), molybdenum (Mo), boron (B), calcium (Ca), antimony (Sb), cobalt (Co), etc. are also need to be removed from domestic waste water. [3]

In waste water treatment, Nanoparticles have been proven beneficial and effective. The unique characteristic of nanoparticles of having high surface area makes its efficient in removing toxic metal ions, disease causing microbes, organic and inorganic solutes from water. Now a days, several new types and classes of nanomaterials are also proved to be efficient for water treatment like metal-containing nanoparticles, carbonaceous nanomaterials, zeolites and dendrimers. [4]

The paper reviews recent advances on different nanomaterials (nanostructured catalytic membranes, nanosorbents, nanocatalysts, bioactive nanoparticles, biometric membrane and molecularly imprinted polymers (MIPs)) with their application in waste water treatment. Nanotechnology has provided various efficient and effective ways for treatment of domestic waste water in a more precise and accurate way on both small and large scale. [5]

1.1. Nanotechnology in Waste Water Treatment

One of the finest and advance ways for waste water treatment nowadays is Nanotechnology. Scientists are still working on further enhancement of the usage of nanotechnology and there are several reasons behind the success of it. [6] Due to the small size of nanoparticles, they have very high absorbing, interacting and reacting capabilities with high proportion of atoms at surface. [7] Nanoparticles can behave as colloid after mixing it with aqueous suspensions. [8]

Energy conservation can be done with the help of nanoparticles due to its small size which can ultimately lead to cost savings. Main advantage of nanoparticles is that they can treat water in depths and any location which is generally left out by other conventional technologies. [9]

Nanoparticles usage cost should be managed according to existing competition in market as water treatment by using nanoparticles has high technology demand. [10] Nanostructured catalytic membranes, nanosorbents, nanocatalysts, bioactive nanoparticles, biomimetic membrane and molecularly imprinted polymers (MIPs) are the various recent advancements on different nanomaterials for removing toxic metal ions, disease causing microbes, organic and inorganic solutes from water. [11]

1.2. Synthesis of Nanoparticles

The use of extremely small particles in all areas of research, including chemistry, biology, medicine, and material science, is known as nanotechnology. The creation of metal and metal oxide nanoparticles with various sizes, shapes, chemical compositions, and disparities is the subject of nanotechnology.

Between 1 and 100 nanometers in size, nanoparticles can be comprised of carbon, metal, metal oxides, or organic material. [12] When compared to their counterpart particles at higher scales, nanoparticles have unique physical, chemical, and biological features. [13] This phenomenon is due to their properties of higher surface area to volume ratio, increased chemical reactivity or stability, improved mechanical strength, etc. [14] One of the fascinating aspects of advanced scientific research is the process for developing nanomaterials and the study of their uses and qualities. In recent years, science and technology have made numerous achievements; in particular, nanotechnology has contributed to the advancement of an innovative concept for synthesising nanosized materials with desired size and shape.

There are different methods to synthesize nanoparticles such as physical, chemical and biological methods. Several conditions like high vacuum, high energy conversion and toxic chemicals are required by Physical and Chemical methods. Chemical synthesis of NPs has a detrimental effect on the environment and is poisonous; however, a biological green methodology has become more necessary.

According to Figure 1, there are two types of nanoparticle synthesis: (i) top down method, and (ii) bottom up method. [15] The top down strategy emphasizes the physical pathway of nanoparticle formation, whereas the bottom up method emphasizes the chemical and biological routes.

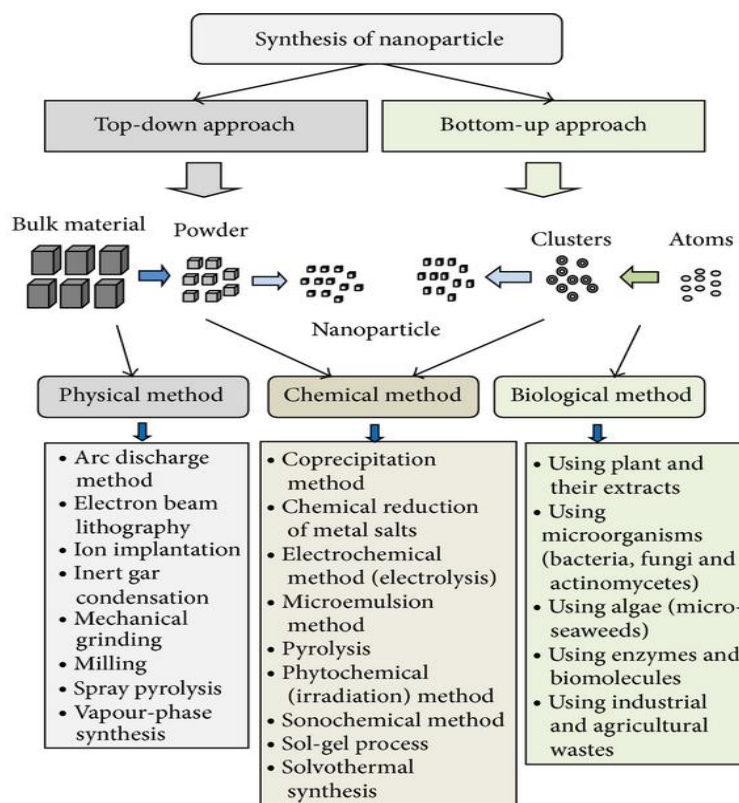


Figure 1: Different synthesis process of nanoparticles

1.3. Green Synthesis of Nanoparticles

Green synthesis is the process of creating materials from environmentally friendly or sustainable sources by using a solvent, a decent reducing agent, and a safe stabilizing ingredient. This synthesis process also yields more stable chemicals and is simple, affordable, predictable, sustainable, and largely repeatable. [17] As a result, scientists are interested in creating a range of nanomaterials through this biosynthetic process, including hybrid materials, bio inspired materials, and metal/metal oxide nanoparticles. Green synthesis is therefore widely accepted as a crucial tool for reducing the harmful effects of traditional nanoparticle production techniques used in labs and industry. In that context, it becomes clear that conventional methods for creating nanoparticles, such as chemical and physical synthesis, are expensive, dangerous, and unfriendly to the environment. [18-25]

However, other aspects of chemically produced nanomaterials, such as size distribution, shape, surface charge, surface chemistry, capping agents, etc., may occasionally have an impact on biological activities. [26, 27] Researchers have identified the precise green pathways, or naturally occurring sources and their products, that may be used to synthesize nanoparticles to address these problems and prevent the negative effects.

Researchers have discovered the exact green routes, or naturally occurring sources and their products, that can be used to make nanoparticles in order to avoid these harmful effects. [28, 29, 30]

1.4. Biological Components of Green Synthesis

Numerous physical and chemical synthesis methods require for high radiation, highly hazardous reductants, and stabilizing agents, all of which can have detrimental impacts on marine life and humans. The green synthesis of metallic nanoparticles, in contrast, is a one-step eco-friendly bio-reduction process that needs only a small amount of energy to start the reaction. [31] The cost-effectiveness of this reduction technique is also very good. Green nanoparticle synthesis can be divided into following categories:

- Phyto approaches, which include using actual plants and plant extracts.
- Using microorganisms like fungus, yeasts (eukaryotes), bacteria, and actinomycetes as part of the microbial method to synthesis.
- Bio-template pathways, such as the use of membranes, viruses, and diatoms as templates. [32, 33]

1.5. Green synthesis copper oxide nanoparticles by plant extracts

Heavy metals have a tendency to build up in different areas of plants in varying amounts. As a result, plant extract-based biosynthetic approaches have drawn more attention as an easy, effective, affordable, and achievable way as well as a great substitute for traditional preparation methods for nanoparticle manufacturing. In a "one-pot" synthesis procedure, a variety of plants can be used to minimize and stabilize metallic nanoparticles.

The rate of metal nanoparticle synthesis with the aid of plant extract is more persistent, significantly faster and extremely mono-dispersive in comparison to other biological methods, such as microorganisms. Additionally, compared to other biosynthetic techniques that are comparable to chemical nanoparticle development, the reaction kinetics of plant-assisted nanoparticle synthesis is substantially faster. Due to the high-quality phytochemicals they produce, plant components such as fruit, leaves, stems, and roots are commonly used for the environmentally friendly method of producing nanoparticles.

To further investigate the various potential uses of metal/metal oxide nanoparticles, numerous researchers have used green synthesis methods to produce the nanoparticles using plant leaf extracts. [34, 35]

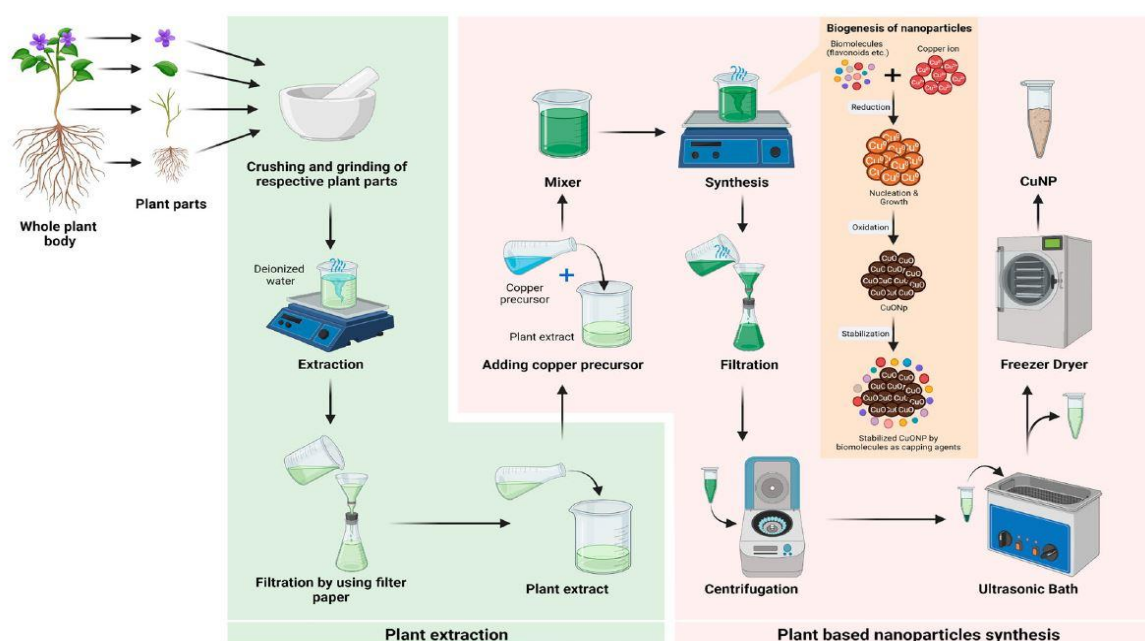


Figure 2: Different steps involved in synthesis of CuO nanoparticles

In the phytosynthesis method, plant extracts are used as a capping and reducing agent during the synthesis of nanoparticles. The creation of CuO-NPs, which are less expensive than other Nobel metals including Ni, Cu, Zn, Au, and Fe, is considered to be a promising method for creating metal oxide nanoparticles. Due to their biocidal qualities, metal oxide NPs such as CuO has gained interest in the biomedical community. These applications include illness treatment, drug delivery, cellular delivery, biomedical imaging, and medication delivery.

Due to the above mentioned facts, numerous plant extracts have been used to produce copper oxide nanoparticles in significant quantities. [36] The metal salt is combined with the plant extracts in this plant-based manufacturing process, and the reaction takes 1-3 hours to finish at room temperature. Flavonoids, phenols, proteins, terpenoids, and tannins are some of the bioactive metabolites found in plant extracts that work as reducing and stabilising agents to turn metallic ions into nanoparticles. The copper salts reduce as a result of the plant extract's production of electrons. When phytochemicals interact with copper ions to cause reduction, copper oxide nanoparticles are produced. [37, 38]

Chapter 2. Literature Review

An environmentally friendly method of producing nanoparticles with unique properties is biosynthesis. Because they are inexpensive and require minimal maintenance, plants are known as the chemical factories of nature. Plants have demonstrated outstanding potential in heavy metal detoxification as well as accumulation, which may be used to overcome environmental toxins as even minute quantities of these heavy metals are dangerous even at very low concentrations.

In comparison to other biological synthesis methods, such as microorganisms, nanoparticle synthesis using plant extract has positive aspects because the rate of metal nanoparticle synthesis with the aid of plant extract is more persistent, significantly faster, and extremely mono-dispersive. Compared to other biosynthetic techniques that are comparable to the generation of chemical nanoparticles, the reaction kinetics of plant-assisted nanoparticle synthesis is substantially faster.

Due to the high-quality phytochemicals they produce, plant components such as fruit, leaves, stems, and roots are commonly used for the environmentally friendly method of producing nanoparticles. Here, using a variety of plant extracts, Copper oxide nanoparticles have been widely synthesized for the aforementioned reasons. The metal salt is combined with the plant extracts in this plant-based manufacturing process, and the reaction takes 1-3 hours to finish at room temperature. Flavonoids, phenols, proteins, terpenoids, and tannins are just a few of the bioactive metabolites found in plant extracts. These substances operate as reducing and stabilizing agents, converting metallic ions into nanoparticles. The copper salts are reduced as a result of the production of electrons by plant extract. When phytochemicals and copper ions interact, reduction takes place and copper oxide nanoparticles are produced.

Copper oxide nanoparticles have stable chemical and physical characteristics, are relatively inexpensive, and are photocatalytic. CuO-NPs may be used as anti-infective agents due to their advantageous crystal morphologies and exceptionally high surface areas. The CuO-NPs' antibacterial effect may be attributed to a few different mechanisms. Due of their positive charge, CuO-NPs may stick to the bacterial cell walls. On the surfaces of microbial cells, carboxyl and amine groups interact with CuO-NPs. As a result, bacteria like *B. subtilis* that have a higher density of these ionic groups on their cell surfaces have a higher affinity for and are more susceptible to CuO-NPs. However, positively charged CuO-NPs have less of an impact on Gram-negative bacteria such as *Proteus* species and *P. aeruginosa*. [39, 40, 41]

Several techniques, such as microwave irradiation, precipitation pyrolysis, and thermal breakdown, have been used to create CuO Nps. The green synthesis of CuO NPs, however, has certain clear benefits. Sustainable chemistry, or "green chemistry," aims to reduce the production of dangerous compounds.

One of the easiest and most environmentally acceptable ways to make metal oxide NPs is by plant-mediated synthesis, which has gained popularity because to its non-toxicity as well as the fact that it is a quick and inexpensive procedure. [42, 43]

Some recent reports on the synthesis of CuO NPs from plant sources include the use of *Saraca indica*, which has fluorescence properties, *Aglaia elaeagnoidea*, which has catalytic and recyclability properties, *Fortunella japonica*, which is used for electro catalytic detection of 4-nitrophenol, Catalytic reduction of 4-nitrophenol is performed by root extract of *Rheum palmatum L.*, waste water treatment is done by *Madhuca longifolia*, mosquito larvicidal activity is controlled by *Tridaxprocumbens* leaf extract and lemon grass tea extract is used for the synthesis of ultra small copper nanoparticles. [44, 45]

Dey et al. studied about the synthesis and characterization of mango leaves biosorbents for removal of iron and phosphorous from contaminated waste water. The optimal preparation of mango leaves as biosorbents for iron and phosphorous sorption processes was associated with the modification in inherent textural and morphological characteristics such as measured by XRD, FTIR, BET and SEM-EDX techniques. The important factor is that the mango leaves do not show any specific change in their adsorption capacity even after reusing for iron and phosphorous removal. The size range of all granular adsorbent particles was varied between (1.54–2.12 μm) and effect of varying degree of agglomeration was also noticed. [46]

Melkamu et al. provided a fast and simple green synthesis method for the synthesis of Copper oxide nanoparticles using non-toxic *Justicia Schimperiana* plant leaf extract (JSPLE) from Ethiopia. Presence of various functional groups responsible for reducing and stabilizing during the biosynthesis process is confirmed by FTIR analysis. From XRD analysis it was confirmed that the synthesized NPs were crystalline in nature with monoclinic structure and the average size of the crystallite particles were found to be 21.8 nm. [47]

Rajabai et al. synthesized Paracetamol- CuO nanoparticles using microwave method. Precursor was prepared using aqueous solution of paracetamol, copper sulphate and NaOH in the molar ratio of 0.1:0.1:0.2 and it was prepared in 100 ml of double distilled UV – treated water. The mixture was constantly stirred for an hour and then heated in a domestic microwave oven (480W, 92⁰C) for 10 mins.

And the precipitate was separated, dried to form CuO NPs. Using X-ray diffraction analysis, particle size of Paracetamol-CuO NPs was determined as 18.527 nm. SEM micrograph of CuO NPs shows well defined, spherical particles of NPs and the grain size is in the range of 20 nm. [48]

CuO NPs were synthesized using the leaf extract of *Justicia adhatoda* and it was observed that the leaf extract has good capability of acting as reducing agent for conversion of Copper ions to CuO NPs. In this method, *Justicia adhatoda* leaf extract and CuCl₂ solution in different concentrations were taken in a beaker and heated for several minutes at room temperature and after few hours formation of NPs started. From the XRD analysis it was noticed that CuO NPs formation faces central to the cubic assembly.

From FESEM analysis, it was observed that size of synthesized NPs was found to be 45.07 nm and is of spherical shape. [49]. An eco friendly technique was adopted by Ijaz et al. to synthesize CuO NPs and to evaluate their antimicrobial, antioxidant and photo-catalytic dye degradation potentials. Aqueous extract of *Abutilon indicum* was used for the synthesis. After successful synthesis of CuO NPs, it was confirmed that NPs with hexagonal, wurtzite and sponge crystal structure was formed. [50]

The leaf extract of *Ocimum basilicum* was used by Katoglu et al. for the synthesis of CuO NPs. Synthesis of NPs was carried out by mixing copper sulphate dehydrate (CuSO₄.5H₂O) with the leaf extract. NPs exhibited antibacterial activity against pathogenic bacterial strains *Escherichia coli* and *Staphylococcus aureus*. Size of the NPs was found to be ranging under 70 nm. [51]

Leaf extract of *Eucalyptus globoulus* was used by Alhalili et al. to synthesize copper oxide nanoparticles. Using SEM analysis, mean particle size of 88 nm was obtained and the average crystalline size was found to be around 85.80 nm was observed by the Debye–Scherrer formula. Crystalline and monoclinic phase of CuO NPs was obtained by this method. Methyl orange was used to investigate the adsorption characteristics of the nano-adsorbents and adsorption efficiency of 95 mg/g was attained at room temperature. [52]

Similar research work was carried out by Sylvia Devi et al. to demonstrate the adsorption capacity of CuO NPs by using leaf extracts of *Centella asiatica* (L.). [53] This technique can be utilized to create copper oxide NPs that can be utilized for the photocatalytic destruction of methyl orange. In the absence of reducing agents, these NPs can convert methyl orange to its leuco form in an aqueous solution.

It is more economical than alternative methods. Because of their small size, copper oxide nanoparticles have a catalytic effect. Because they have a high surface to volume ratio, nanoparticles have more active sites than bulk materials. Such produced copper oxide nanoparticles have effective catalytic capabilities.

Mahmoud et al. prepared two samples of CuO NPs by using extracts of mint leaves and orange peels. For the elimination of Pb(II), Ni(II), and Cd(II) using CuO NPs, several batch experiment parameters, including nanosorbent dose, contact time, pH, and initial metal concentration, were taken into consideration. [54]

In this study by Hassan et al., the modified sol-gel process is used to create copper oxide nanoparticles. Its surface was examined and characterized using a variety of methods, including XRD, SEM, TEM, and AFM. The presence of CuO is indicated by all of the reflection peaks from the XRD study, and the spectrum showed that the particle size produced was around (21.11 nm), which was in agreement with estimates from SEM and TEM.

CuO examination using SEM, TEM, and AFM revealed that the particle sizes are in the nanometer range. Through the use of an adsorption batch approach, these oxides were employed to separate Cd (II) and Ni (II) ions from their aqueous solutions (binary system). [55]

Tsegaye et al. reported the synthesis of CuO NPs using aqueous extract of *Prunella vulgaris* flower. Synthesized NPs were crystalline in nature with spherical shape and average particle size is in the range of 41 – 76 nm. FCC structure of the particles was reported by XRD analysis.

The biomolecules and functional groups found in NPs, however, were identified via FTIR analysis. This study further highlights the fact that CuO NPs made using green technique show effective antibacterial activity against the tested strains of *S. aureus* and *K. pneumoniae*. Therefore, CuO NPs antibacterial activity has demonstrated the biological importance of NPs and will be important in the search for new treatments to address the problem of these organisms developing drug resistance. [56]

Keabadile et al. synthesized CuO NPs using leaves of *Terminalia phanerophlebia*. Green and traditional chemical methods were adopted for the synthesis. SEM images revealed that synthesized nanoparticles were spherical in shape with agglomerated particles. From Zeta Potential analysis it was known that green synthesized CuO have more negative surface charge than chemical synthesized CuO. UV-vis spectroscopy revealed that green synthesized CuO NPs have higher conductivity than the traditional chemically synthesized nanoparticles. [57]

Some of the copper oxide nanoparticle synthesis methods adopted by different researchers have been covered in the above literature. Synthesis methods and experimentation provided in this thesis work is unique due to some of the reasons mentioned below:

- Membrane study is done on a pilot scale basis in order to observe the efficiency of nanoparticles in industrial scale.
- In this research work synthesis of CuO NPs is done using the leaves extracts of *Artocarpus heterophyllus* which is not widely studied by many researchers.
- Simulated wastewater was used where sewage effluent was collected from nearby sewage pumping station and mixed with Cr⁺⁶ solution in order to mimic real Cr+6 infested wastewater.

- Reusability study of treated effluent was carried out in seed germination of mustard seeds. Most of the studies either concentrate on treatment or on reusability but complete study is conducted here.
- Ceramic membrane is used for removal of organic matter, turbidity as well as separate nanoparticles.
- Industrial scale of study will be done in order in future to further complete the thesis work.

Chapter 3. Materials and methods

3.1. Materials and Equipment Used

3.1.1. List of Apparatus

- Weighing Machine (Sartorius, Germany, 0.0001-220gm)
- Magnetic Stirrer (Remi, India)
- Centrifuge Machine (Tarsons, India)
- Tube Furnace (K.Furnace, India)
- Ultrafiltration Membrane (Johnson, India)
- Two Pressure Gauges (Micron, India)
- Peristaltic Pump (Kisan Kraft, India)

3.1.2. List of Chemicals

- Copper Sulphate ($\text{CuSO}_4 \cdot 5\text{H}_2\text{O}$) (GR, India)
- Sodium Hydroxide (NaOH) (GR India)
- Ethanol ($\text{CH}_3\text{CH}_2\text{OH}$) (GR India)

3.1.3. Plant Used

- **General Name:** Jackfruit
- **Scientific Name:** *Artocarpus heterophyllus*
- **Source of Collection:** Jadavpur University Campus



Figure 3: Membrane filtration Pump Setup



Figure 4: Jackfruit tree (*Artocarpus heterophyllus*)

3.2. Methodology

CuO NPs was synthesized by the Green Synthesis Method and proper precursors were used during the synthesis of nanoparticles. The synthesized nanoparticles were characterized by XRD, FTIR, FESEM & EDS, UF membrane study, Seed germination study. Chromium was taken as a specimen metal to prepare the metallic solution. The specimen metallic solution was used to study the metal removal capacity of CuO NPs prepared by green synthesis.

3.2.1. Green Synthesis of CuO NPs

3.2.1.1. Preparation of Precursors

Copper Sulphate pentahydrate ($\text{CuSO}_4 \cdot 5\text{H}_2\text{O}$) was taken as the main source of Copper in CuO NPs for our study.

- Molecular Weight of $\text{CuSO}_4 \cdot 5\text{H}_2\text{O}$ is:
(63.546 + 32.06 + 4 X 16 + 5*(1.00794*2 + 15.9994)) = 249.68 grams.
- To prepare 1 M solution of $\text{CuSO}_4 \cdot 5\text{H}_2\text{O}$, 159.61 gm of $\text{CuSO}_4 \cdot 5\text{H}_2\text{O}$ (S) was weighed and dissolved in distilled (deionized) water. The solution was stirred with a stirring rod until it is completely dissolved.
- The solution is then diluted with distilled water to get the final volume of 1000 ml. Prepared Copper Sulphate solution was kept in a glass container for further use.

0.1M Sodium Hydroxide (NaOH) solution was prepared as (NaOH) solution acted as the precipitating agent in our synthesis.

- Molecular weight of NaOH is (23+16+1) =40 grams.
- 0.4 grams of Sodium hydroxide pellets were weighed and dissolved in distilled (deionized) water. The solid was stirred with a stirring rod until it completely dissolved.
- The solution is then diluted with distilled water to get the final volume of 100ml and stirred again to get homogeneous. Prepared Sodium hydroxide solution was kept in a glass container for further use.

During green synthesis of nanoparticles, *Artocarpus heterophyllus* leaf extract along with small amount of NaOH (0.1M) was used as a precipitating agent.

- *Artocarpus heterophyllus* (Jackfruit) leaves were collected and washed with distilled water several times in order to remove any kind of surface dirt.
- The leaves were then left in open atmosphere for the removal of trace amount of water present on the surface of the leaves.
- The dried leaves are boiled and phytochemicals were extracted which acted as reducing agent in the synthesis of nanoparticles.

- The extract was filtered using Whatman 42 filter paper and kept in for further use.

3.2.1.2. Synthesis of Nanoparticles

- CuSO₄ solution was taken in a Borosil 250 ml conical flask and it was mixed thoroughly with the help of a magnetic stirrer.
 - Leaf extract that was prepared earlier, added drop wise in the CuSO₄ Solution in systematic manner and stirred at 900 rpm.
 - NaOH was added to the solution in a drop wise at a regular interval.
 - All the steps regarding the synthesis of copper oxide nanoparticles were taking place at room temperature. ($28 \pm 2\text{ }^{\circ}\text{C}$).
 - The solution turned brownish from colour less and deep brown precipitate was formed at pH 8.
 - The precipitate is then repeatedly washed with the help of distilled water to remove any traces of dirt and alkali.
 - The resultant precipitate was kept for sometime undisturbed for the heavy portion to settle down at the bottom of the flask. And the excess non useful portion of the precipitate was expelled out. The useful portion was centrifuged and was heated in tube furnace (JAY CRUCIBLES, India) at around 500°C for 15 mins.
 - After that the heated material was collected from the furnace and left in open atmosphere to cool down. Then, the material was hand grinded using mortar-pestle.
- The resultant nanoparticles were stored for further use.

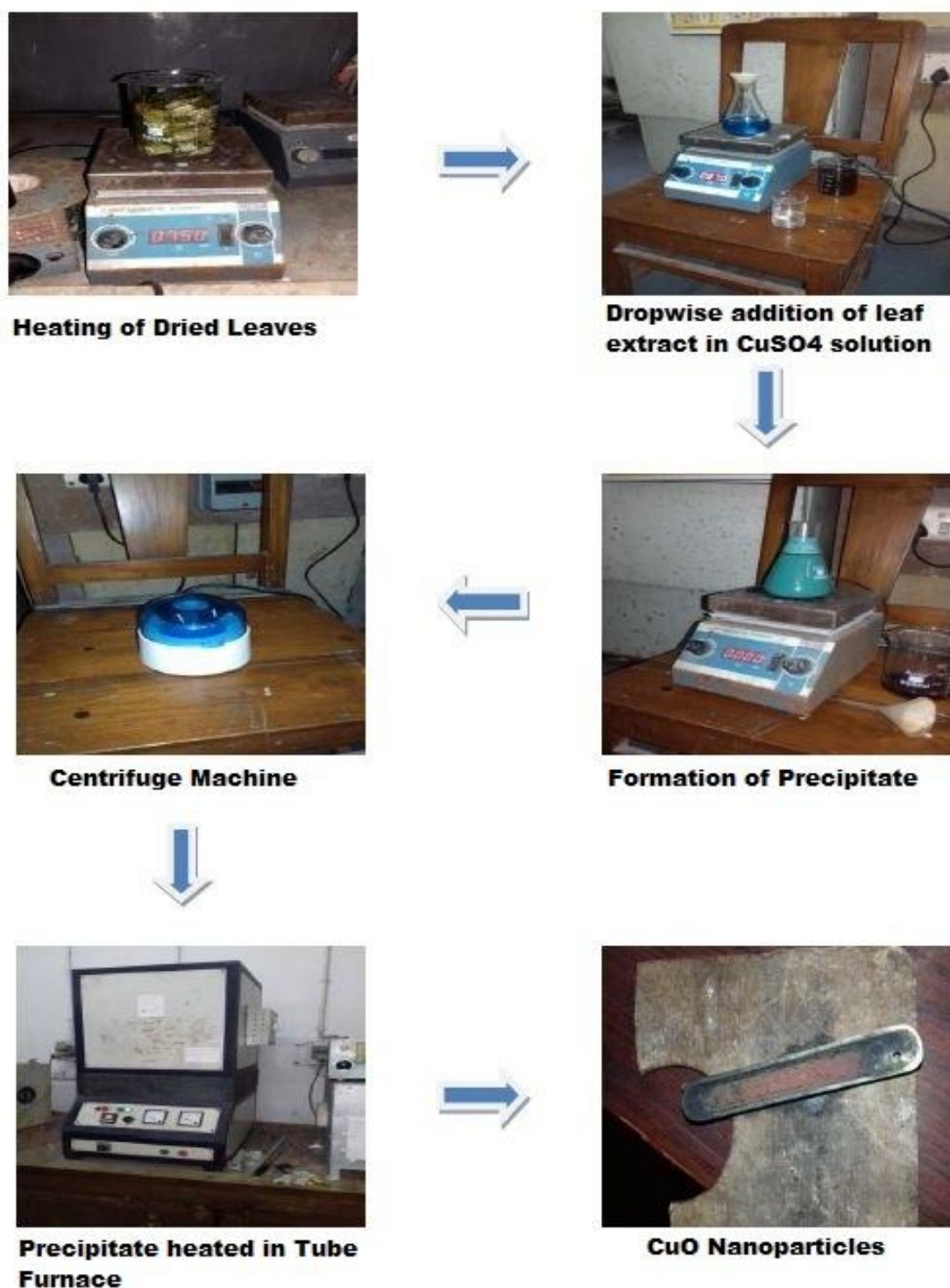


Figure 5: Schematic diagram of different steps involved in synthesis of copper oxide nanoparticles

3.2.2. Chromium removal study

3.2.2.1. Application of CuO NPs in Chromium removal

In the batch adsorption studies, carried out for the adsorption of Chromium ions by CuO NPs, the maximum amount of metal ions adsorbed by the nanoparticles is calculated by performing Batch Equilibrium study which is carried out by varying different parameters like Dose of nanoparticles, Concentration of Chromium metal solution, pH of Chromium metal solution and the contact time between the nanoparticles and metallic solution.

Chromium removal capacity of synthesized CuO NPs is determined by using the following equation:

$$\% \text{ Removal} = \left(\frac{C_o - C_t}{C_o} \right) \times 100$$

Where, C_o is the initial concentration of Chromium solution in ppm

C_t is the final concentration of Chromium solution after adsorption in ppm

3.2.2.2. Preparation of dichromate solution

Chromium is taken as the specimen heavy metal to continue the current research study. A 100 ppm chromium solution was prepared. 282.8 mg of Chromium powder was weighed and added in 1000 ml of distilled water and stirred. Distilled water was added to the solution to make a final solution of volume 1000 ml. Solution of chromium was obtained by diluting the 100 ppm stock solution. These solutions were preserved to carry on further study.

3.2.2.3. Equilibrium Study

To perform the equilibrium study, Dichromate solution weighing 100 ml (pH 2) was taken in a 250 ml Erlenmeyer flask and ml of synthesized CuO NPs at 10 gm/L was added to the solution and kept undisturbed for 24 hrs. About 81% removal rate was obtained. After that the solution was centrifuged and the supernatant was collected. The CuO NPs adsorbed with Chromium metal ions were further studied by FESEM & EDS and FTIR.

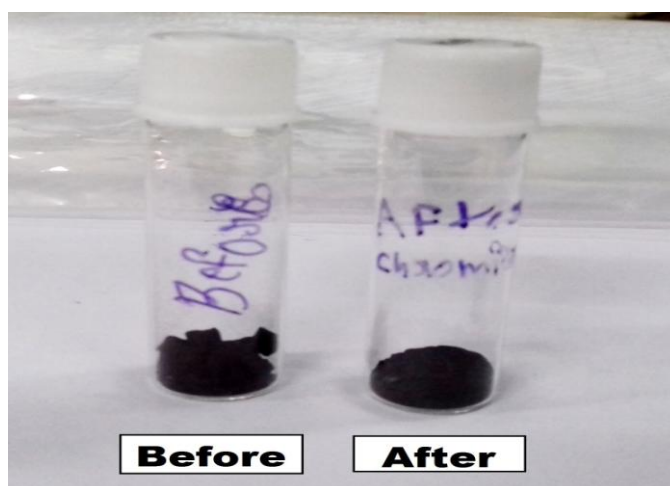


Figure 6: Green synthesized CuO NPs (before and after adsorption of chromium)

3.2.2.4. Kinetic Study

To perform the kinetic study, required amount of specimen dichromate solution was taken in Erlenmeyer flask and desired dose of CuO NPs were added subsequently. The flask was added in a magnetic stirrer to agitate the solution throughout the experiment at a fixed rpm. At a fixed time interval of (5, 10, 20, 30, 45, 60 mins), small amount of dosed solution was removed and centrifuged to get the supernatant. This supernatant was used to study the efficiency of synthesized CuO NPs in removing heavy metal. The process was carried out by different combinations of dose, contact time, Initial dye concentration (ppm) and pH of the dichromate solution.



Figure 7: Kinetic Study Experiment

Chapter 4. Characterization of Materials

4.1. FTIR spectroscopy

An analytical method known as Fourier Transform Infrared Spectroscopy, or FTIR Spectroscopy also known as FTIR Analysis is used to distinguish between organic, polymeric, and occasionally inorganic materials. The FTIR analysis method scans the samples and examines chemical characteristics using infrared light.

An essential system in organic chemistry that can pinpoint certain functional groups present in the molecule is infrared or IR spectroscopy. Additionally, the distinct collection of absorption bands can quickly identify the properties of pure chemicals and identify particular contaminants. On the basis that molecules vibrate at particular frequencies, infrared spectroscopy operates. These wavelengths (between 4000 and 200 cm^{-1}) are part of the infrared spectrum. When IR radiation strikes a sample, it absorbs frequencies that are similar to the frequencies of its molecular oscillation and transmits other frequencies. [58]

A plot of absorbed energy against frequency, known as the "infrared spectrum," can be created by using an infrared spectrometer to identify the frequencies of absorbed radiation. A specific molecule can be recognized because diverse materials have different vibrations and produce different infrared spectra. The N atoms in a nonlinear molecule move in $3N-6$ vibrational movements, often known as fundamental vibrations or normal modes. Only molecules that are IR active (or that absorb IR light) have vibrations that are visible in the IR spectrum. A change in the vibrating molecule's dipole moment is required for a mode to be IR active. As a result, the IR spectra do not show symmetric vibration. The vibrations symmetric with respect to the core of a molecule's symmetry are IR inactive. But since all of these are asymmetric molecule, vibrations are IR active; they all show up in the spectrum. [59]

As a result, all chemical groups found in the substance are detected simultaneously. It's interesting that this method is able to quickly detect water molecules and amino acids, which are difficult to detect by other spectroscopes. Chemical groups have a persistent dipole, such as polar bonds, display significant infrared absorption and as a result, the carbonyl groups on polypeptide chains create absorption peaks in the IR spectra of proteins. In mid IR region (4,000 to 1,000 cm^{-1}), main vibrations observed are:

- 1) Stretching vibrations: These are the vibrations along the bonds, and cause changes in length of the bonds.
- 2) Bending vibrations: These cause changes in the bond angle. Involvement of d (in plane) and p (out of plane) vibrations takes place.

An established method for quality control when assessing industrially produced materials is FTIR spectroscopy, which is frequently used as the initial step in the material testing process. A change in the material's composition or the presence of contamination is clearly shown by a change in the distinctive pattern of absorption bands. Visual inspection may reveal imperfections in the product, and FTIR microanalysis is often used to pinpoint their source. Smaller particles, usually 10 to 50 microns in size, as well as greater surface areas can be chemically analyzed using this method.

FTIR analysis is used to:

- Identification and characterization of unknown materials (e.g., films, solids, powders, or liquids)
- Identification of contamination on or in a material (e.g., particles, fibers, powders, or liquids)
- Identification of additives after extraction from a polymer matrix
- Identification of oxidation, decomposition, or uncured monomers in failure analysis investigations.



Figure 8: IR Prestige-21 FTIR measuring instrument

4.2. XRD

X-ray powder diffraction (XRD) is a fast analytical method that may identify the size of unit cells and is mostly used to determine a crystalline material's phase. Finely powdered, homogenized material is used for the analysis and the average bulk composition is calculated.

The important parameter upon which X-ray diffraction is based upon is the constructive interference between monochromatic X-rays and the crystalline sample. X-rays are produced by cathode ray tube, which are then undergoes filtration to produce monochromatic radiation, which are then focused by collimation, and pointed at the sample. When the circumstances of the process are in accordance with Bragg's Law ($n\lambda=2d \sin \theta$), diffracted rays are produced by the interaction of the incident rays with the sample and results in constructive interference.

This law establishes a connection between the lattice spacing and diffraction angle in a crystalline sample and the wavelength of electromagnetic radiation. Then, these diffracted X-rays are identified, examined, and recorded. Due to the powdered material's random orientation, all potential lattice diffraction directions should be obtained by scanning the sample through a range of 2θ angles. Each mineral has a specific set of d-spacings, hence converting the diffraction peaks to d-spacings enables mineral identification. This is often accomplished by comparing the d-spacings with accepted reference patterns. [60]

The production of X-rays in an X-ray tube is the foundation of all diffraction techniques. The sample is hit with these X-rays, and the diffracted rays are captured. The angle between the incident and diffracted rays is a crucial factor in all types of diffraction.

The most frequent application of X-ray powder diffraction is the detection of unidentified crystalline materials (such as minerals and inorganic chemicals). Studies in geology, environmental science, material science, engineering, and biology depend on the identification of unknown solids.

Other applications include:

- Characterization of crystalline materials
- Identification of fine-grained minerals such as clays and mixed layer clays that are difficult to determine optically
- Determination of unit cell dimensions
- Measurement of sample purity.

Debye-Scherrer equation is used to calculate the crystallite size using XRD data, Crystallite Size:

$$D = \frac{0.9\lambda}{\beta \cos \theta}$$

where, D is the dimension(measured) of the particle in the direction perpendicular to reflecting plane

k= Scherrer constant (crystallite shape factor with approximate value of 0.95),

λ = wavelength of the used X-ray beam (1.54184 \AA or 0.154184 nm),

β = Full width at half maximum (FWHM) of the peak in radian, and

θ = Bragg diffraction angle.

The XRD analysis for the present study was carried out in SmartLab SE (Rigaku Corporation, Japan) XRD machine.



Figure 9: SmartLab SE XRD measuring instrument

4.3. FESEM & EDS

One of the most versatile and well known analytical techniques for analyzing the surface of specimen is Field emission scanning electron microscopy (FE-SEM). An electron microscope offers advantages including high magnification, large depth of focus, high resolution and ease of sample preparation when compared to conventional optical microscope.

Electron gun generates electrons which enter the surface of a sample and inelastic interaction with the atoms in the sample occur which results in the formation of various signals. These signals contain the information about the surface morphology and composition.

The specimen generates various low energy secondary electrons and the intensity of these secondary electrons is governed by the surface morphology of the sample. Construction of the image of sample surface takes place by measuring secondary electron intensity as a function of the position of the scanning primary electron beam.

Applications of FESEM

- Measurement of sample microscopic features
- Study of surface morphology
- Characterization of coatings
- Integrated circuit evaluation
- Fine structural analysis
- Study of microstructures
- Fracture and structural defects analysis

Energy-dispersive X-ray spectroscopy (EDS or EDX) is an analytical method that analyses the chemical characterization, composition and elemental analysis of materials. A material that has been activated by an energy source (such the electron beam of an electron microscope) releases a core-shell electron that helps to release part of the energy that has been absorbed. [61,62]

The difference in energy is subsequently released as an X-ray with a distinctive spectrum depending on its parent atom while a higher energy outer-shell electron moves in to take its place. As a result, it is possible to analyze the composition of a sample volume that has been excited by an energy source. The location of the peaks in the spectrum helps to identify the element, whereas the signal's strength reflects the element's concentration.

Applications of EDS

- Investigations of failures and determination of their causes
- Analysis of flaws and defects in products
- Identifying, restricting, and detecting contaminants
- Quality assurance of raw materials and finished goods



Figure 10: FESEM and EDS measuring instrument

4.4. Ultrafiltration (UF) Membrane Study

Ultra filtration (UF) is a membrane filtration procedure that forces water through a semi-permeable membrane element using hydrostatic pressure. The driving force behind the membrane is a pressure difference.

The water can pass through the membrane's pores because of the different pressures. All material that is larger than the pores is retained on the membrane's surface. Pore size exclusion is the term for this procedure. The membrane is referred to be semi-permeable because it retains some substances while allowing water to pass through. [63,64]

Filtration study was performed in the cross flow membrane filtration (CMF) mode at various transmembrane pressures (TMP) on the pilot scale set up. Prior to the experimental run, membranes were conditioned by immersing in distilled water overnight to obtain a stabilized flux right from the beginning of the experiment. Permeate flow was monitored by regulating the control valve at the retentate flow path. TMP was varied from 1-3 bar. Time study was conducted for 120 min. Permeate was collected at regular intervals at fixed TMP of 2 bar and CFV of 3ml/min.

4.4.1. Procedure

To carry out this study, 20 L SS setup is used. This setup is comprise of a feed tank (20L) made up of high grade steel, a peristaltic pump, inlet and outlet pressure gauges, electric stirrer and UF ceramic membrane developed from 80% Clay and 20% Alumina of 10/7 inner and outer diameter respectively.

10 L waste water is poured into the feed tank and nanoparticles (10 gm/L) are added. To study the chromium removal capacity of the nanoparticles, 500 ml of 5ppm chromium solution was added to the feed tank.

4.4.2. Specification

- Outer diameter of membrane: 10 mm
- Inner diameter of membrane: 7 mm
- Pump capacity: (RPM: 800 – 1200 , Pressure: 10-40 kg/cm²)
- Pressure Gauges: Pressure: Max 150 kg/cm²

4.4.3. Wastewater characterization

- **Chemical Oxygen Demand (COD)**

The capacity of water to consume oxygen during the breakdown of organic materials in the water is measured by the term "chemical oxygen demand," or COD. To explain it in a different way, it's the quantity of oxygen required to oxidize organic matter contained in a given volume of water.

The indirect measurement of pollutants in waste water can be done with the help of COD analysis. It can be used to measure the quantity of oxidizable contaminants present in waste water, efficacy of waste water treatment.

- **Biochemical Oxygen Demand (BOD)**

The amount of oxygen consumed by bacteria and other microorganisms during the aerobic decomposition of organic matter at a particular temperature is termed as Biochemical Oxygen Demand (BOD). It is used to predict the amount of organic pollution present in an aquatic system. It is also used by medical industry to determine oxygen consumption for cell culture.

- **Turbidity**

Turbidity is a measurement of the amount of light scattered by the components of water when light is passed through a water sample. It is an optical property of water. With the increase in intensity of scattered light, the turbidity also increases. Material that causes water to be turbid include clay, silt, algae, dissolved colored organic compounds and other microscopic organisms. Turbidity is measured in Nephelometric turbidity units (NTU).

- **Total Suspended Solids (TSS)**

Total suspended solids can be defined as the amount of particulate matter in a water sample that can be entrapped by filter. If TSS is high, it will be difficult for light to travel through the water and the plants, algae will not be able to grow. It is often described as a measure of conductivity, salinity, alkalinity and hardness of water.

4.5. Seed Germination Study

There are two types of Chromium: Cr (III) and Cr (VI). Cr (VI) is more mobile, hazardous to living things, and has mutagenic and carcinogenic effects. Due to Cr (VI)'s greater solubility, it considerably raises the risk of stomach and lung cancer.

Chromium with high percentage in the soil gets absorbed and build up in the above-ground sections of plants, then enter the food chain, impacting human health either directly or indirectly. Additionally, it hinders the growth, enzyme activity, photosynthesis, metabolism, biomass production, and crop productivity of the plants. Phosphate and sulphate routes are used by roots to absorb Cr (VI). In contrast to Cr (III), which is transported through an inactive channel, it is then easily transferred to other areas of the plant. Roots play a major part in the accumulation and transfer of Cr since they are the first plant organs to be exposed to it in the soil.

Chromium results in reduced growth, photosynthesis, mineral nutrients and crop productivity. Cr also affects other physiological processes such as seed germination and enzyme activity. [65]

4.5.1. Procedure

To carry out the study, seeds of black mustard seeds were collected. Seeds of uniform size, colour and weight were collected for experimental work. The seeds were surfaced sterilized using 0.1% mercuric chloride and washed with distilled water. The seeds were kept in petridish covered with soaked filter paper. 25 seeds were kept in each petridish and soaked in respective water designated as:

C-Control (distilled water)

Cr+6 -5ppm Cr+6

Cr+6 T-Treated Cr+6 with nanoparticles in batch study

I-R-Initial untreated simulated effluent (sewage effluent +5ppm Cr+6)

P-Permeated from membrane study

The seeds were observed for 72 h in terms of % seed germination and root/shoot length

The germination percentage is expressed as percentage of germinated seeds to the total number of viable seeds that were tested by following formula: [66,67]

$$[\%G = (\text{Number of germinated seeds} / \text{Total number of planted seeds}) \times 100]$$

Stress tolerance index is used for determining the high yield and stress tolerance potential of genotypes. Stress tolerance indices for different growth parameters were calculated using following formulae []:

$$[RLSTI = (\text{Root length of stress plant} / \text{Root length of control plant}) \times 100 \text{ (3)}]$$

$$[SLSTI = (\text{Shoot length of stress plant} / \text{Shoot length of control plant}) \times 100]$$

Chapter 5. Results and Discussion

Characterization of CuO NPs

Synthesized CuO NPs were characterized using different characterization techniques. Inspect F50 (FEI, USA) FESEM machine studied the particles size, outline, and morphology of nanoparticles. IRPrestige-21 FTIR Machine set up was used for recording FT-IR spectra, which identify bioactive molecules. The crystalline nature, structure and average size of CuO NPs were determined by the SmartLab SE XRD set up.

5.1. FTIR

FT-IR analysis is mostly used system to detect structural properties of material of the sample. Presence of probable bioactive molecules is due to decrease of copper ions and the capping ability of copper oxide nanoparticles. The FT-IR absorption spectra were used to identify the presence of different functional groups of the active components (CuO NPs) based on the peak value in the region of infrared radiation. The FTIR spectra of control leaf extract (after reaction with CuSO₄) and synthesized CuO NPs (after adsorption of Chromium) are shown in Fig.

The broad and strong peak at around 3588.8 cm⁻¹ can be attributed to the O-H groups of alcohols and phenols. This peak shifted to lower field at 3392.7 cm⁻¹ in the synthesized CuO NPs. The band at 1387.4 cm⁻¹ is assigned to C-H stretching. The peaks observed in the range of 793.2-1620.9 cm⁻¹ have been assigned to alcohols and phenolic groups, C-N stretching vibrations of amines. The major peak was observed to be 505.4 cm⁻¹ should be a stretching of Cu-O. The similar results have been reported in literature where CuO NPs was synthesized using different leaves extracts.

FTIR operation was carried out at an operating at a resolution of 4000–400 cm⁻¹ in the absorbance mode. The absorbance data was transformed in to percentage Transmittance using Beer-Lambert law. Various absorbance bands of synthesized CuO NPs, as observed in FTIR analysis are given below:

Table 1: FTIR functional groups

Frequency Range (cm^{-1})	Appearance	Group	Compound Class
3588.8, 3574.7	Medium, sharp	O-H Stretching	Alcohol
3491.3, 3392.7, 3492.7, 3393.8	Strong, broad	O-H Stretching	Alcohol and intermolecular bonded
2064.4	Strong	N=C=S stretching	Isothiocyanate
1620.9, 1625.6	medium	C=N stretching	Imine/oxime
1387.4, 1395.3	medium	C-H bending	Alkane
1112.4	strong	C-O Stretching	Secondary Alcohol
999.9, 981.4, 883.8, 793.2, 893.2	strong	C=C bonding	Alkene
637.5, 603.9, 505.4, 596.7, 498.8	strong	CuO Stretching	Inorganic

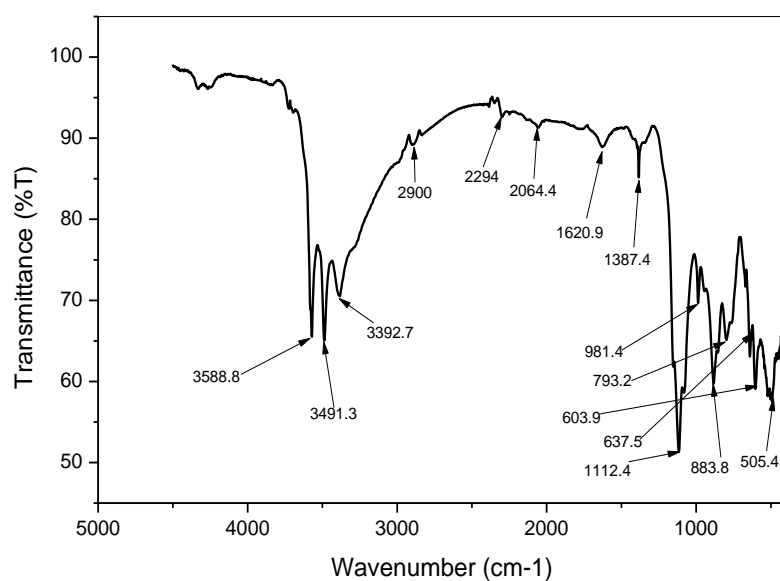


Figure 11: FTIR of CuO NPs (Before biosorption)

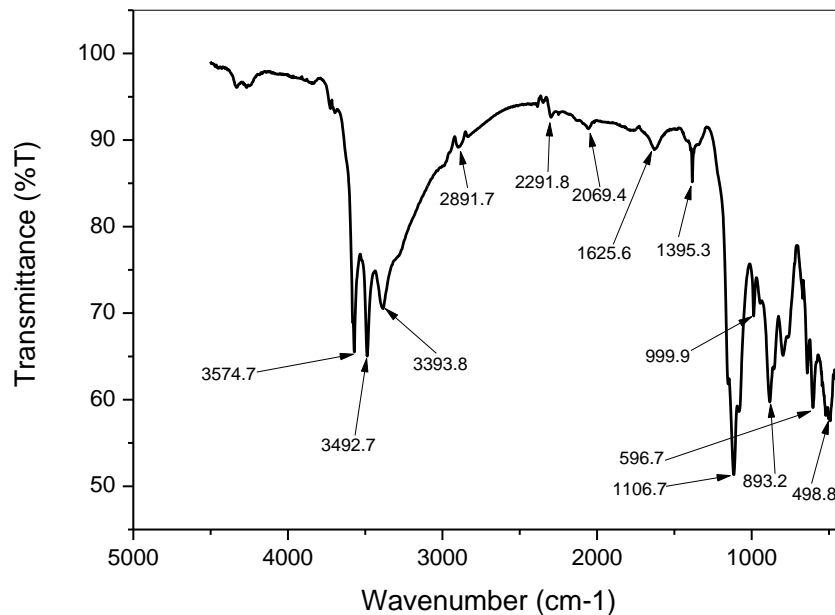


Figure 12: FTIR of CuO NPs (After biosorption)

5.2. XRD

X-ray diffractometer with $\text{CuK}\alpha$ as radiation source and 1.5406 \AA wavelength, confirmed the production of CuO -NPs. To analyze the crystalline structure and phase of copper oxide, the XRD method was used in the 2θ range of 20 - 80 . The sample's XRD examination was conducted according to the following standards.

Step: 0.01° ; Speed: $0.4/\text{min}$; Mode: XRF reduction (1D scan).

The phase purity and crystalline nature of the synthesized CuO Nps were examined using XRD analysis. Major diffraction peaks at 2θ values of 22.789 , 35.541 , 38.733 , 48.792 , 58.634 , 61.563 , 66.302 were assigned to the (020) , (002) , (111) , $(\bar{2}02)$, (202) , $(\bar{1}13)$ and (022) miller indices planes, respectively. CuO Nps have a distinct peak at $2\theta = 38.733^\circ$ with the diffraction of the (111) plane, indicating that they are monoclinic crystals with the space group $C2/c$ (15). The results of the XRD examination show that the synthesized CuO Nps are monoclinic and crystalline materials.

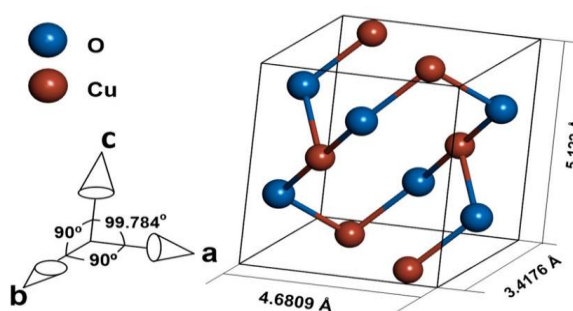


Figure 13: Crystal Structure of CuO NPs

The allocated lattice parameters, $a = 4.684 \text{ \AA}$, $b = 3.425 \text{ \AA}$, and $c = 5.129 \text{ \AA}$, were in good agreement with the reference JCPDS No. (5-661). The size of the crystalline nanoparticles was determined using the Debye–Scherrer formula for the maximum intensity peak.

On the basis of the highest 2θ peak, we calculated the crystalline size to be 16.092 nm for CuO Nps. Also, due to the smaller crystalline size, the XRD pattern appears noisy.

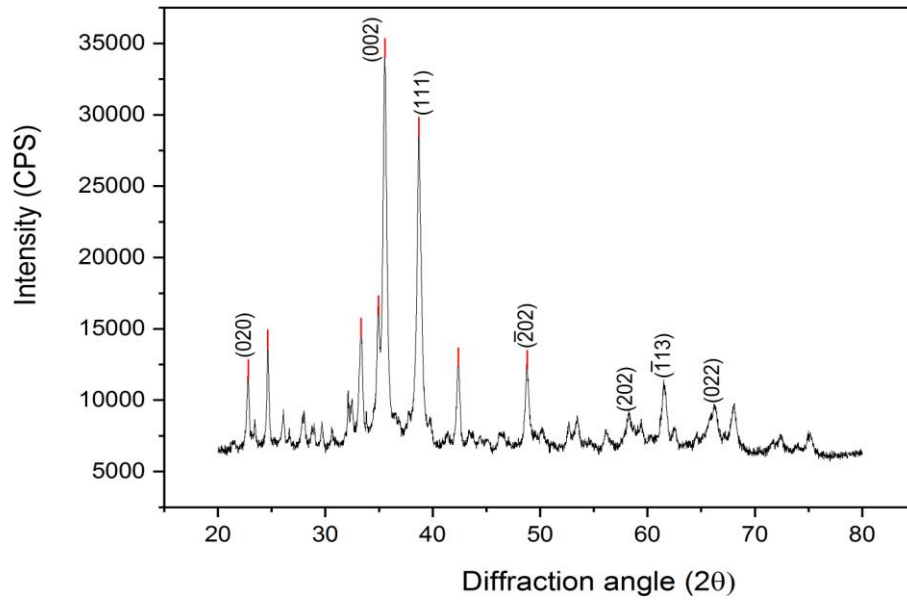


Figure 14: XRD of green synthesized CuO NPs

Table 2: Crystalline Size from XRD data

2θ (degree)	FWHM (deg) (β)	d-spacing (angstrom)	hkl	Crystalline Size(nm)	Lattice Parameter (a) Å
22.7891	0.249	1.5406	020	32.5462	3.081
35.5416	0.40622	2.523	002	20.539	5.046
38.7337	0.5227	2.323	111	16.109	4.023
48.7922	0.3986	1.866	$\bar{2}$ 02	21.875	5.277
58.6343	1.5102	1.581	202	6.032	4.471
61.5633	0.5975	1.505	$\bar{1}$ 13	15.475	4.991
66.3026	133.0398	1.41	022	0.071	3.988
Average				16.092	4.411

5.3. FESEM and EDS

FE-SEM was used to assess the surface morphological characteristics of the synthesized CuO NPs. According to the FE-SEM image in Figure (15,17) the produced CuO NPs have a distinct spherical form. It has been discovered that the biological synthesis of CuO NPs results in relatively smaller, homogeneous-dimension, quasi-spherical particles. The slight aggregation in the produced nanoparticles could be due to the use of biological components during the synthesis process.

To confirm the elemental composition, the energy dispersive x-ray spectroscopy (EDX) is a popular analysis to find element percentage and also ensure of impurity interrupted when it was performed. In EDX analysis, before adsorption of chromium, the peak of copper was found almost 71.60 % weight and peaks of oxygen was found almost 15.30 % weight. And after adsorption of chromium, the peak of copper and oxygen was found almost 62.16 % and 0.05% weight respectively and peaks of Chromium was found almost 0.11 % weight.(Fig. 16,18)

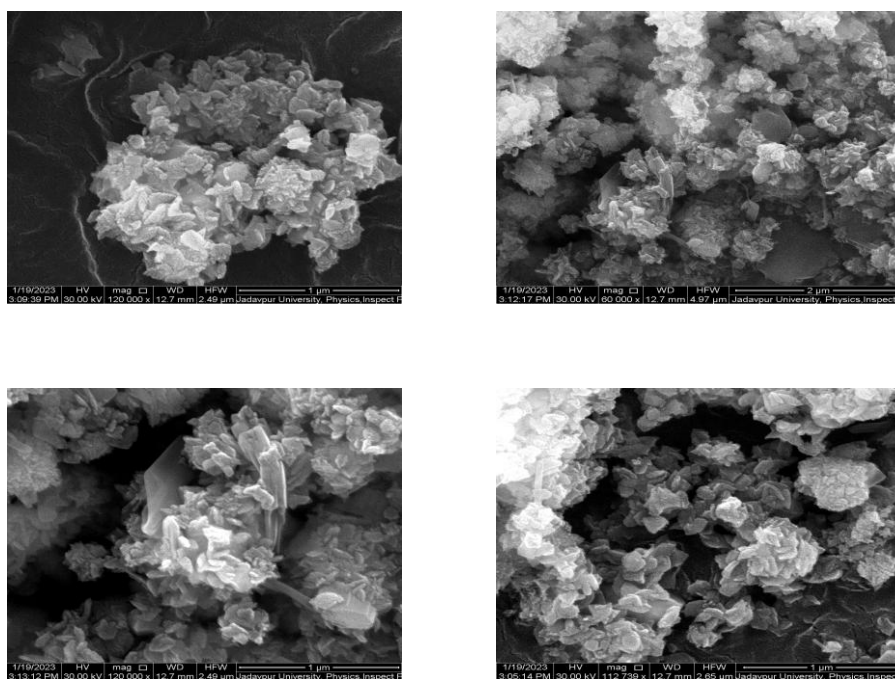


Figure 15: FESEM images of CuO NPs (Before biosorption)

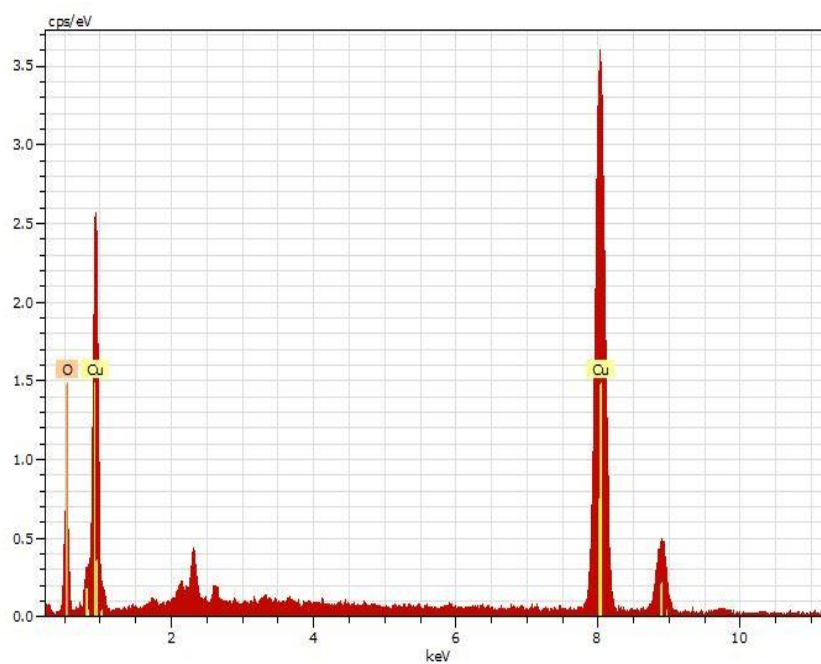


Figure 16: EDS of CuO NPs (Before biosorption)

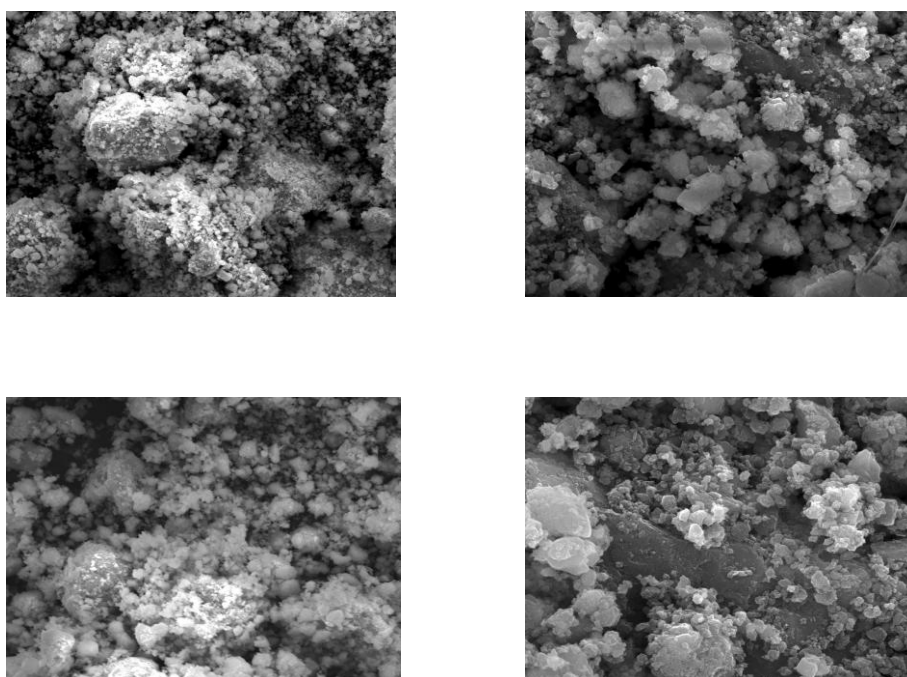


Figure 17: FESEM images of CuO NPs (After biosorption)

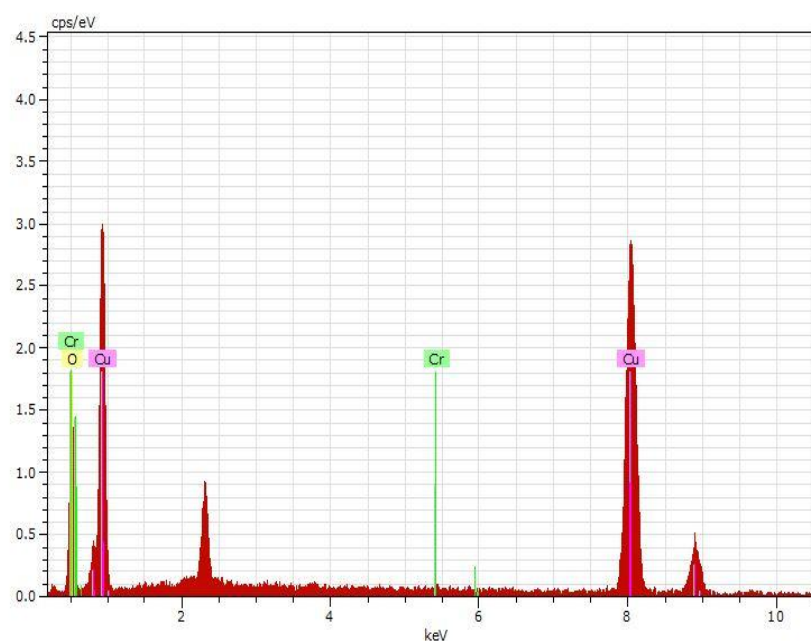


Figure 18: EDS of CuO NPs (After biosorption)

5.4. Removal study of Cr (VI) using CuO NPs

5.4.1. Effect of adsorbent dose

The performance of adsorption is significantly impacted by the dose of nanosorbents. CuO NPs were utilized at various dose concentrations (5, 10, and 20 gm/L) to test their effectiveness in removing chromium metal ions. Figure 19 illustrates that the capacity of nanoparticles to remove chromium increases as the dose of nanosorbents increases. The complexity of the metal ions and the availability of more binding sites on the surface of nanosorbents are the causes.

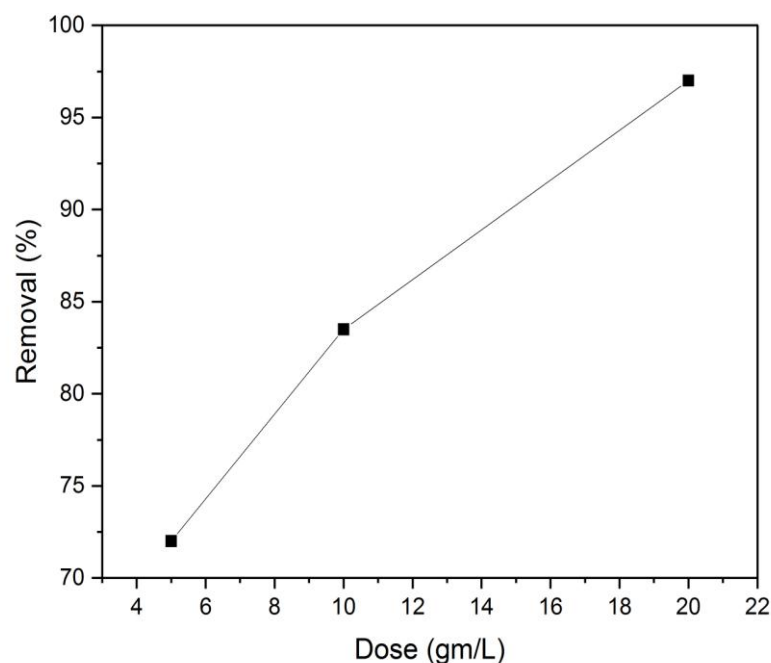


Figure 19: Adsorbent dose versus removal

5.4.2. Effect of Contact time

Figure 20 illustrates the efficiency of synthesized CuO NPs in removing chromium metal, which required 60 min of contact time to attain equilibrium. After 60 minutes, it was seen that the adsorption rate had little effect on it and was almost fixed. This can be due to the studied nanosorbents' saturation capacity. Chromium was removed with a percentage of 95% in 60 minutes, 88% in 45 minutes, 81% in 30 minutes, 68% in 20 minutes, 55% in 10 minutes, and 50% in 5 minutes.

Highest percentage of heavy metal removal capacity of synthesized CuO NPs is obtained due to the presence of high intensity of surface functional groups of CuO nanoparticles. The reason behind that can be the richness of the extract obtained from the leaves of *Artocarpus heterophyllus* with various phytochemical constituents.

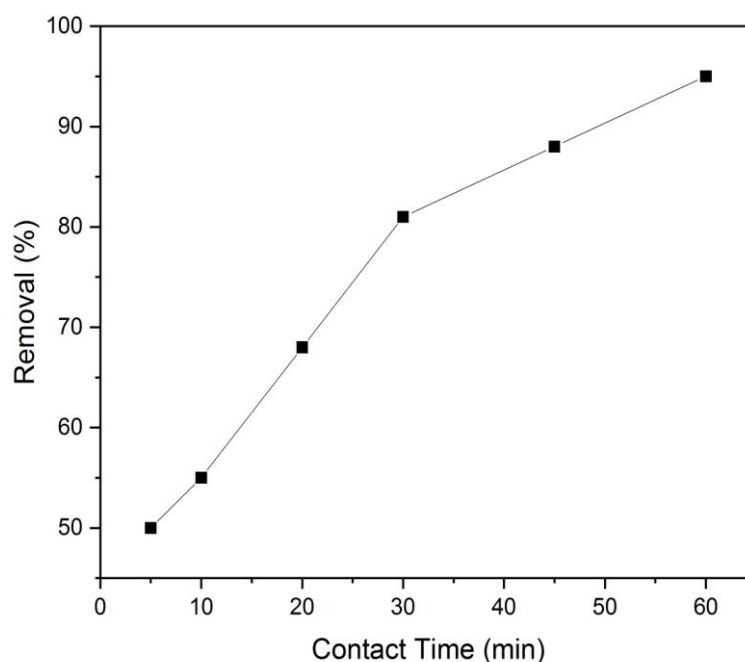


Figure 20: Contact time versus removal

5.4.3. Effect of initial concentration of Dichromate Solution

The chromium removal percentage decreases with increasing the concentration of the chromium metal ions, as illustrated in Figure 21 with regard to the adsorption of the metal ions at various concentrations. At a given nanoparticle dose of 10 gm/L and pH 2, the percentage removal of chromium was obtained at 99%, 95%, 83%, 64%, and 47% for various metal concentrations (1, 5, 10, 15, and 20 ppm).

This is because there are more absorbable empty sites available at low metal concentrations, and as a result, there are more metal ions present on the nanosorbent. As the amount of accessible adsorption sites decreases with increasing metal ion concentration, so does the rate at which these metal ions are removed.

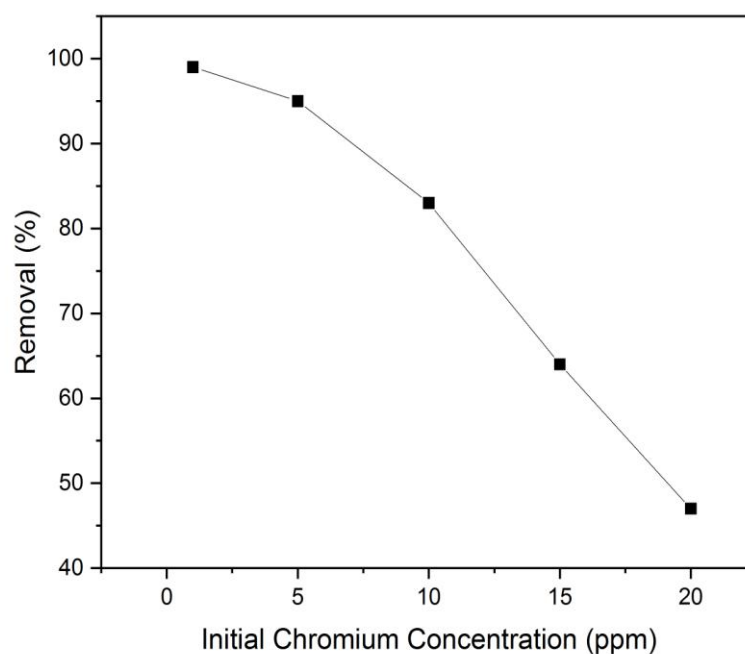


Figure 21: Initial chromium concentration versus removal

5.4.4. Effect of pH

Removal of heavy metals from contaminated water depends largely on the pH of the solution. At a fixed nanoparticle dose of 10 gm/L and Chromium metal concentration of 5 ppm, with pH Values (2,4,6) the respective heavy metal removal efficiency obtained were 93.5%, 73%, 56%. Chromium removal increased with the increase in pH range from 2 to 6. (Fig. 22)

The highest adsorption was observed at pH 6, which could be due to the protonation of functional groups on Copper oxide NPs. The pH value of 2 was chosen as the optimum pH based on the present analysis.

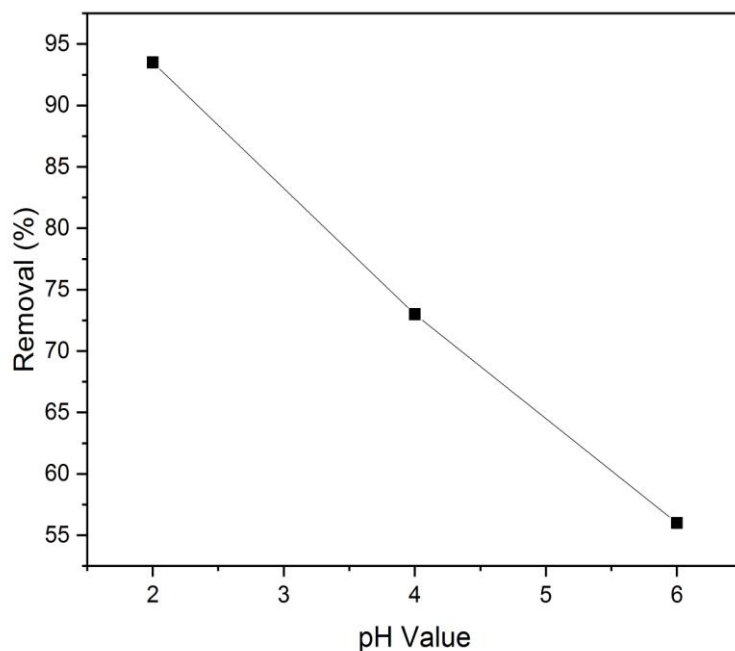


Figure 22: pH value versus removal

5.5. Ultrafiltration Membrane study

5.5.1. Flux versus Time Study

The variation of the permeate flux of the effluent as a function of time is shown in Figure 23. All experiments were carried out at 2 bar TMP using the UF membrane. The permeate flux of effluent obtained was around 150 LMH at 30 min of operation. The flux initially increased from 88 LMH to 150 LMH for 30 mins after which a steady state flux was achieved at 60 min with 151 LMH. Flux then reduced to 130 LMH at 120 min. This may be due to pore blocking with nanoparticles which further decreased the flux. However, the blockage was temporary and reversible in nature and the membrane could be regenerated by backwashing with clean water only.

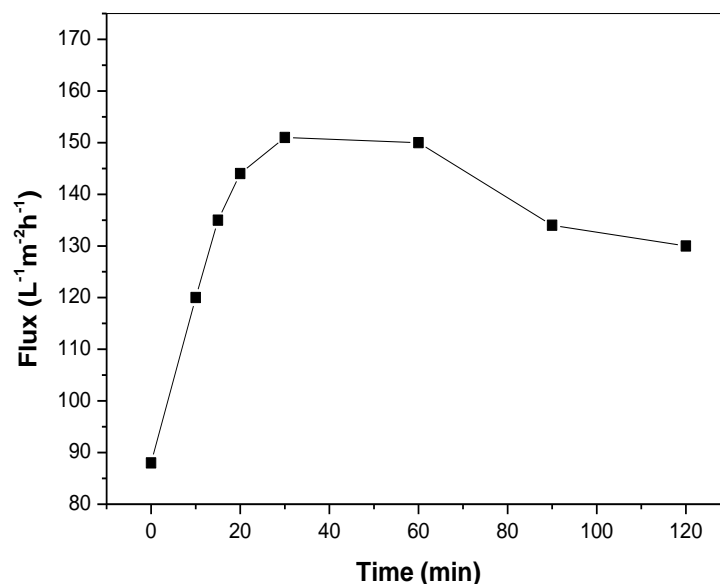


Figure 23: Graph showing Flux versus Time study

5.5.2. Flux versus Transmembrane Pressure Study

Increasing the TMP resulted in increase in flux where flux value of 94-190 LMH was obtained for TMP 1-3 respectively. (Fig. 24)

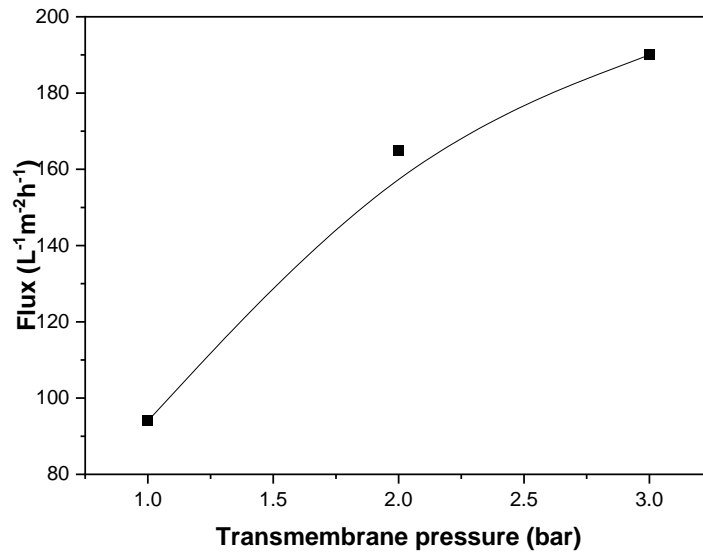


Figure 24: Graph showing Flux versus Transmembrane pressure study

Table 3: Waste water characterization (before and after membrane study)

	Initial	Final
COD	449 ppm	27 ppm
BOD	38 ppm	Not detected
Turbidity	110 NTU	< 1 NTU
TSS	88 ppm	2 ppm

5.6. Effect of chromium on mustard seed germination

5.6.1. Effect of different un-treated and treated solutions on seed germination

The result of present study reveals that 72% seeds were germinated when exposed to 5 ppm Cr^{+6} solutions within 24 H and no further seeds were germinated in next 72 h. But nanoparticle treated Cr^{+6} showed an increase in germination to about 80%. Similar effect was also observed with simulated wastewater where only 68% seeds were germinated after 24 h and no further seeds germinated. Permeated exposed seeds showed germination at par to control with 96% seed germination after 72 h.



Figure 25: Study of seed germination (24 Hrs)

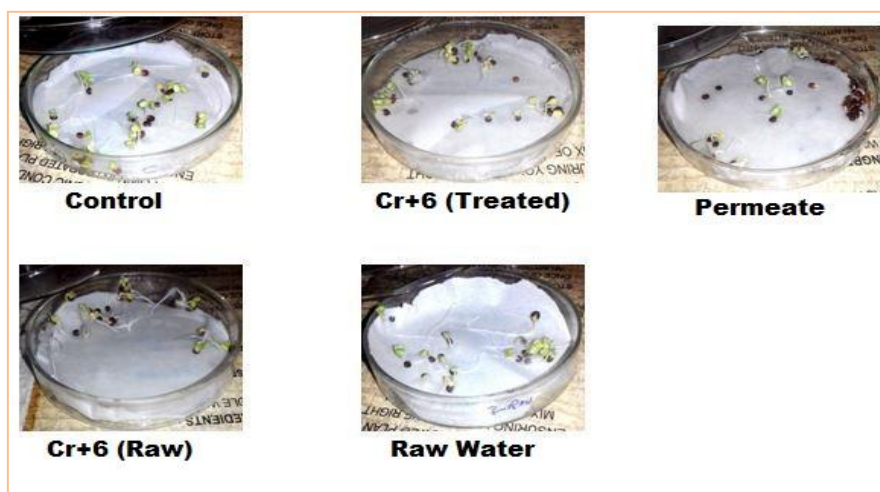


Figure 26: Study of seed germination (48 Hrs)



Figure 27: Study of seed germination (72 Hrs)

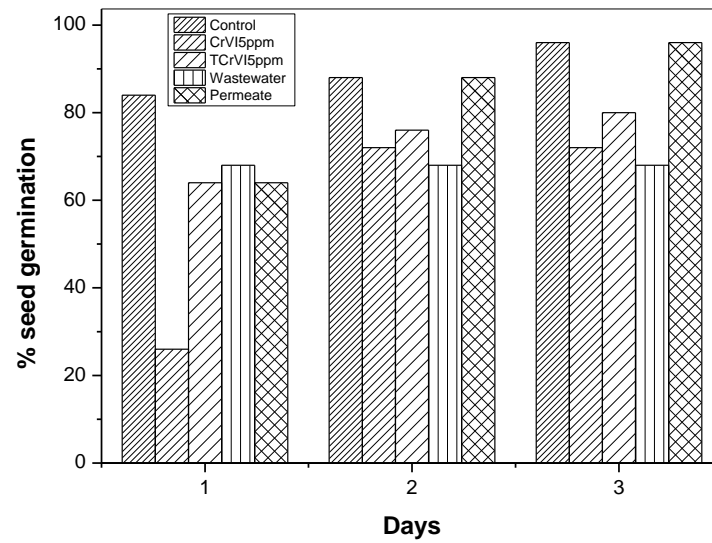


Figure 28: Percent seeds germinated w.r.t days

5.6.2. Toxicity on Root and Shoot Elongation

The results after 72 h of exposure showed decreased root length for Cr+6 of about 0.2 cm+ 0.02 as compared to control of about 0.8cm+ 0.03 respectively. Cr+ showed lowest tolerance level of about 26% after 24h that increased to 60% after 72. Treated Cr+6 on the other hand showed tolerance level of 75%. Permeate exposed seeds have tolerance value of 98%.

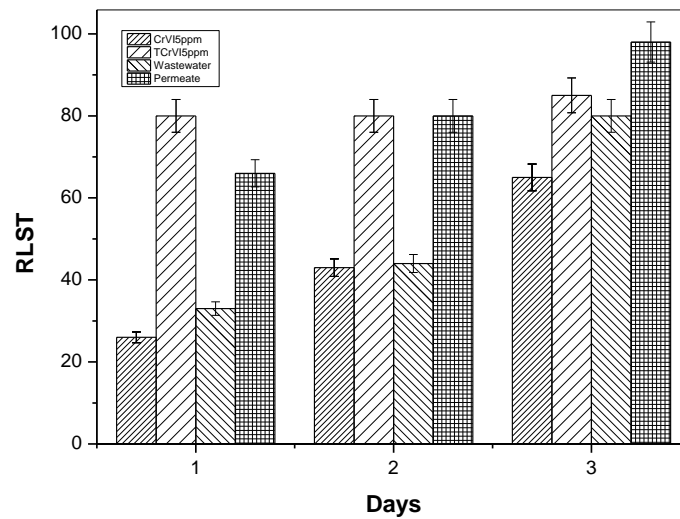


Figure 29: RLST w.r.t days

Chapter 6. Conclusion

The following study is done to understand and analyze the different synthesis methods and characterization of Copper Oxide nanoparticles. Heavy metal removal capacity of the synthesized nanoparticles was also examined during the present study. Dichromate solution was used as model heavy metal solution in this research work.

1) XRD analysis of synthesized CuO NPs showed sharp peaks corresponding to planes (020), (002), (111), ($\bar{2}02$), (202), ($\bar{1}13$) and (022) confirmed the monoclinic structure of CuO. The average crystallite size (using Debye-Scherrer formula) was found to be 16.092 nm.

2) The FTIR test confirmed the presence of bioactive molecules present in the synthesized CuO NPs. It also confirmed different function group and physical interaction of macromolecules with CuO NPs.

3) FESEM results confirmed the nano range of CuO nanoparticles. Results also confirmed their spherical shape. Results from EDX were consistent with the FESEM results and it was evident from the EDS spectrum that the CuO nanoparticles were synthesized successfully. The major constituents of the nanoparticles before adsorption of chromium were Cu (71.60%) and O (15.30%). After adsorption, constituents were Cu (62.16%), Cr (0.11%) and O (0.05%) respectively.

It was also confirmed from the EDX results that the CuO NPs were crystalline, based on their strong, intense, narrow width and sharp peaks in the EDX spectrum.

4) Cr (VI) removal capacity of synthesized CuO NPs was also studied by varying the parameters like adsorbent dose, initial chromium concentration, pH of dichromate solution and contact time.

5) Flux value of 150 LMH was obtained after 30 min of operation after which there was a decline of about 13% in flux due to deposition of nanoparticles. Considerable removal of organic matter was achieved along with Cr+6 in membrane combined nanoparticle study.

6) Permeate exposed mustard seeds showed 96% seed germination with root and shoot length comparable to control.

After analyzing the results from the above tests it was concluded that CuO NPs are highly efficient in removing heavy metal (Chromium) from the waste water.

Chapter 7. Future Scope

In terms of applying synthesized nanoparticles for waste water treatment and purification, some important future perspectives must be considered:

- 1) For the use of these green-synthesized copper oxide nanoparticles in industrial and commercial scales, further thorough studies are needed to examine the sustainability and toxicity issues. However, using nanomaterials might also lead to secondary contamination, therefore this important problem needs to be addressed and thoroughly investigated.
- 2) Although the synthesis of these CuO NPs is environmentally friendly, certain crucial and difficult aspects need to be examined and optimized, such as the effects of reaction parameters and stability problems, as these elements can change the behavior of nanoparticles, their morphologies, and their efficacy in removing heavy metal.
- 3) The synthesized nanoparticles can be reused and this study of synthesis of NPs can be further repeated in various other ways. The synthesized CuO NPs can be further applied in real industrial projects in order to remove heavy metal from the waste water of various industries like tannery waste from Leather manufacturing industries which are the major source of Chromium pollution.
- 4) Direct measurement of nanoparticle size, grain size, size distribution and morphology can be done with the help of TEM analysis. BET analysis can be undertaken in order to get the surface area and porosity distribution of the synthesized nanoparticles.

References

- [1] I. Gebremedhn, M. Kahsay and M. Aklilu, "Green Synthesis of CuO Nanoparticles Using Leaf Extract of *Catha edulis* and Its Antibacterial Activity," *J. Pharm. Pharmacol.*, vol. 7, pp. 327-342, 2019.
- [2] A. Pradeep, M. Dinesh, A. Govindaraj, D. Vinothkumar and N. Ramesh Babu, "Phytochemical analysis of some important medicinal plants," *Int J Biol Pharm Res.*, vol. 5, pp. 48-50, 2014.
- [3] M. Islam, M. Khatun, M. Rahman and M. Alam, "Green synthesis of copper oxide nanoparticles using *Justicia adhatoda* leaf extract and its application in cotton fibers as antibacterial coatings," *AIP Adv.*, no. 1:125223., 2021.
- [4] R. Sivaraj, P. Rahman, P. Rajiv, H. Abdul Salam and R. Venckatesh, "Biogenic copper oxide nanoparticles synthesis using *Tabernaemontana divaricate* leaf extract and its antibacterial activity against urinary tract pathogen.," *Spectrochim. Acta A Mol. Biomol.*, no. 133:178–81, 2014.
- [5] E. Mohamed, "Green synthesis of copper & copper oxide nanoparticles using the extract of seedless dates," *Heliyon.*, vol. 6, no. e03123., 2020.
- [6] r. M. Nasee, R. Ramadan, J. Xing and N. Samak, "Facile green synthesis of copper oxide nanoparticles for the eradication of multidrug resistant *Klebsiella pneumonia* and *Helicobacter pylori* biofilms," *Int. Biodeterior. Biodegradation.*, no. 159:105201, 2021.
- [7] R. Naik, S. Stringer, G. Agarwal, S. Jones and M. Stone, "Peptide templates for nanoparticle synthesis derived from polymerase chain reaction-driven phage display.," *Adv. Funct. Mater.*, vol. 14, pp. 25-30, 2002.
- [8] T. Premkumar and K. Geckeler, "Nanosized CuO particles via a supramolecular strategy," *Small.* 2(5), pp. 616-620, 2006.
- [9] G. Ren, D. Hu, E. Cheng, M. Vargas-Reus, P. Reip and R. Allaker, "Characterisation of copper oxide nanoparticles for antimicrobial applications," *Int J Antimicrob Agents* 33(6), pp. 587-590, 2009.
- [10] R. R. P and M. B. N, "Compendium of Indian medicinal plants," *Journal of Central Drug Research Institute*, vol. 15, p. 19, 1994.
- [11] S. S, R. H, Goddard, G. K and F. Bielmyer, "Comparative effects of dissolved copper and copper oxide nanoparticle exposure to the sea anemone, *Exaiptasia pallida*," *Aquatic Toxicology*, vol. 160, pp. 205-213, 2015.
- [12] A. Chatterjee, R. Sarkar, A. Chattopadhyay, P. Aich, R. Chakraborty and T. Basu, "A simple robust method for synthesis of metallic copper nanoparticles of high antibacterial

- potency against E. coli.," *Nanotechnology* 2012,, vol. 23, 2012.
- [13] M. Grigore, E. Biscu, A. Holban, M. Gestal and A. Grumezescu, "Methods of synthesis, properties and biomedical applications of CuO nanoparticles.," *Pharmaceuticals*, vol. 9, no. 75, 2016.
- [14] V. Rintu, H. Joy Prabu and I. Johnson, "Green Synthesis and Characterizations of Flower Shaped CuO Nanoparticles for Biodiesel Application.," *Sens. Transducers J.*, vol. 210, pp. 38-41, 2008.
- [15] B. Cristiano José de Andrade, L. Maria de Andrade, M. Anita Mendes and C. Augusto Oller do Nascimento, "An Overview on the Production of Microbial Copper Nanoparticles by Bacteria, Fungi and Algae.," *Double Blind Peer Reviewed International Research Journal Publisher: Global Journals Inc.* 17, 2017.
- [16] S. Sumitha, R. Vidhya, M. Lakshmi and K. Prasad, "Leaf extract mediated green synthesis of copper oxide nanoparticles using Ocimum tenuiflorum and its characterization.," *Int. J. Chem. Sci*, no. 14, pp. 435-440, 2016.
- [17] M. Grigore, E. Biscu, A. Holban, M. Gestal and A. Grumezescu, "Methods of synthesis, properties and biomedical applications of CuO nanoparticles," *Pharmaceuticals* 2016, no. 9, p. 75, 2016.
- [18] H. Amin., B. Arain Ahmed, F. Amin and M. Suriho Ali, "Phytotoxicity of Chromium on Germination, Growth and Biochemical Attributes of Hibiscus esculentus," *American Journal of Plant Sciences*, vol. 4, pp. 2431-2439, 2013.
- [19] D. Wilkins, "A technique for measurement of Lead Tolerance in Plants," *Nature*, vol. 180, pp. 37-38, 1957.
- [20] A. Azam, A. Ahmed, M. Oves, M. Khan and A. Memic, "Size-dependent antimicrobial properties of CuO nanoparticles against Gram-positive and -negative bacterial strains.," *International journal of nanomedicine*, no. 7, 2012.
- [21] M. Ponnar, C. Thangamani, P. Monisha, S. Gomathi and K. Pushpanathan, "Influence of Ce doping on CuO nanoparticles synthesized by microwave irradiation method," *Applied Surface Science*, no. 449, pp. 132-143, 2018.
- [22] P. Singh, P. Kumar, M. Hussain, A. Das and G. Nayak, "Synthesis and characterization of CuO nanoparticles using strong base electrolyte through electrochemical discharge process," *Bulletin of Materials Science*, no. 39, pp. 469-478, 2016.
- [23] S. Vishnu, P. Ramaswamy, S. Narendhran and R. Sivaraj, "Potentiating effect of ecofriendly synthesis of copper oxide nanoparticles using brown alga: antimicrobial and anticancer activities.," *Bulletin of Materials Science*, no. 39, pp. 361-364, 2016.
- [24] A. Ullah, N. Ullah and S. Rasheed, "Green synthesis of copper nanoparticles using extract of Dicliptera Roxburghiana, their characterization and photocatalytic activity against

- methylene blue degradation," *Letters in Applied NanoBioScience*, no. 9, pp. 897-901, 2020.
- [25] F. Kiessling, Z. Liu and J. Gätjens, "Advanced nanomaterials in multimodal imaging: Design, functionalization and biomedical applications.," *Journal of Nanomaterials*, 2010.
- [26] S. Usha, K. Ramappa, S. Hiregoudar, G. Vasanthkumar and D. Aswathanarayana, "Biosynthesis and Characterization of Copper Nanoparticles from Tulasi (*Ocimum sanctum* L.) Leaves.," *International Journal of Current Microbiology and Applied Sciences*, no. 6, pp. 2219-2228, 2017.
- [27] J. Jayaprakash, N. Srinivasan and P. Chandrasekaran, "Surface modifications of CuO nanoparticles using Ethylene diamine tetra acetic acid as a capping agent by sol-gel routine," *Spectrochimica Acta Part A: Molecular and Biomolecular Spectroscopy*, no. 123, pp. 363-368, 2014.
- [28] Z. Kayani, M. Umer, S. Riaz and S. Naseem, "Characterization of Copper Oxide Nanoparticles Fabricated by the Sol–Gel," *Method. Journal of Electronic Materials*, no. 44, pp. 3704-3709, 2015.
- [29] A. Abdul Majeed, A. Abd, A. Hussein and N. Habubi, "Fabrication and Characterization of Copper Oxide Nanoparticles/PSi Hetero diode.," *International Letters of Chemistry, Physics and Astronomy*, no. 57, pp. 25-35, 2015.
- [30] V. Moses, "Biological Synthesis of Copper Nanoparticles and its impact-a Review.," *Researchgate.Net.*, no. 3, pp. 28-38, 2016.
- [31] D. Mott, J. Galkowski, L. Wang, J. Luo and C.-J. Zhong, "Synthesis of Size-Controlled and Shaped Copper Nanoparticles," *Am. Chem. Soc*, no. 23, pp. 5740-5745, 2007.
- [32] J. K. Sharma, M. S. Akhtar, S. Ameen, S. Pratibha and S. Gurdip, "Green synthesis of CuO nanoparticles with leaf extract of *Calotropis gigantea* and its dye-sensitized solar cells applications.," *J. Alloys Compd.*, no. 632, pp. 321-325, 2015.
- [33] J. Peternela, M. F. Silva, M. F. Vieira, R. Bergamasco and A. M. S. Vieira, "Synthesis and Impregnation of Copper Oxide Nanoparticles on Activated Carbon through Green Synthesis for Water Pollutant Removal.," *Mater. Res.*, no. No. e20160460., p. 21, 2018.
- [34] P. Afshin, M. Mir Fazlollah and R. Mohammad Safi, "Fabrication of anchored copper oxide nanoparticles on graphene oxide nanosheets via an electrostatic coprecipitation and its application as supercapacitor," *Electrochim. Acta*, no. 88, pp. 347-357, 2015.
- [35] M. R. Mohammad Shafiee, M. Kargar and M. Ghashang, "Simple Synthesis of Copper Oxide Nanoparticles in the Presence of Extractive *Rosmarinus Officinalis* leaves.," *J. Nanostruct.*, no. 6, pp. 28-31, 2016.
- [36] N. Tamaekong, C. Liewhiran and S. Phanichphant, "Synthesis of Thermally Spherical

- CuO Nanoparticles.," *J. Nanomater*, no. No. 507978, 2014.
- [37] N. Verma and N. Kumar, "Synthesis and Biomedical Applications of Copper Oxide Nanoparticles: An Expanding Horizon.," *ACS. Biomater. Sci. Eng.*, no. 5, pp. 1170-1188, 2019.
- [38] M. Altikatoglu, A. Attar, F. Erci, C. Cristache and I. Isildak, "Green synthesis of copper oxide nanoparticles using *Ocimum basilicum* extract and their antibacterial activity," *Fresenius Environ. Bull.*, no. 25, pp. 7832-7837, 2017.
- [39] S. Sathiyavimal, S. Vasantharaj, D. Bharathi, M. Saravanan, E. Manikandan, S. Kumar and A. Pugazhendhi, "Biogenesis of copper oxide nanoparticles (CuONPs) using *Sida acuta* and their incorporation over cotton fabrics to prevent the pathogenicity of Gram negative and Gram positive bacteria. J. Photochem.," *Photobiol. B Biol.*, no. 188, pp. 126-134, 2018.
- [40] U. Khatoon, K. Mantravadi and G. Rao, "Strategies to synthesise copper oxide nanoparticles and their bio - applications," *A review. Mater. Sci. Technol.*, no. 34, pp. 2214-2222, 2018.
- [41] S. Mohan, Y. Singh, D. Verma and S. Hasan, "Synthesis of CuO nanoparticles through green route using Citrus limon juice and its application as nanosorbent for Cr(VI) remediation: Process optimization with RSM and ANN-GA based model," *Process. Saf. Environ. Prot.*, no. 96, pp. 156-166, 2015.
- [42] M. Nasrollahzadeh and S. Sajadi, "Green synthesis of copper nanoparticles using *Ginkgo biloba* L. leaf extract and their catalytic activity for the Huisgen (3 + 2) cycloaddition of azides and alkynes at room temperature," *J. Colloid Interface Sci.*, no. 457, pp. 141-147, 2015.
- [43] M. Din and R. Rehan, "Synthesis, Characterization, and Applications of Copper Nanoparticles.," *Anal. Lett.*, no. 50, pp. 50-62, 2017.
- [44] G. Wang, G. Wang, X. Liu, J. Wu, M. Li, J. Gu, H. Liu and B. Fang, "Different CuO Nanostructures: Synthesis, Characterization, and Applications for Glucose Sensors.," *J. Phys. Chem. C*, no. 112, pp. 16845-16849, 2008.
- [45] S. Hameed, B. Abbasi, M. Ali, A. Khalil, B. Abbasi, M. Numan and Z. Shinwari, "Green synthesis of nanoparticles through plant extracts: Establishing a novel era in cancer theranostics.," *Mater. Res. Express*, no. 6, 2009.
- [46] Y. Suresh, S. Annapurna, A. Singh and G. Bhikshamaiah, "Green synthesis and characterization of tea decoction stabilized copper nanoparticles," *Int. J. Innov. Res. Sci. Eng. Technol.*, no. 3, pp. 11265-11270, 2014.
- [47] P. Khanna, S. Gaikwad, P. Adhyapak, N. Singh and R. Marimuthu, "Synthesis and characterization of copper nanoparticles.," *Mater. Lett.*, no. 61, pp. 4711-4714, 2007.

- [48] D. Subhashish, S. Anduri, V. G.T.N., P. M. A.V. and H. N., "Synthesis and characterization of mango leaves biosorbents for removal of iron and phosphorous from contaminated water," *Applied Surface Science Advances*, no. 11, pp. 15-20, 2022.
- [49] W. M. Walelign and G. F. Eskedar, "Green Synthesis of Copper Oxide Nanoparticles Using Leaf Extract of *Justicia Schimperiana* and their Antibacterial Activity," *REsearch Square*, pp. 16-24, 2022.
- [50] A. Alemu, B. Lemma, N. Gabbiye, M. T. Alula and M. T. Desta, "Removal of chromium (VI) from aqueous solution using vesicular basalt: A potential low cost wastewater treatment system," *Heliyon*, vol. e00682., no. 4, pp. 22-24, 2018.
- [51] J. I. Md., K. M. T. and R. R. Md., "Green synthesis of copper oxide nanoparticles using *Justicia adhatoda* leaf extract and its application in cotton fibers as antibacterial coatings," *AIP Advances*, no. 11, pp. 1-8, 2021.
- [52] I. Faheem, S. Sammia, A. K. Shakeel, A. Waqar and Z. Sabah, "Green synthesis of copper oxide nanoparticles using *Abutilon indicum* leaf extract: Antimicrobial, antioxidant and photocatalytic dye degradation activities," *Tropical Journal of Pharmaceutical Research*, no. 16(4), pp. 743-753, 2017.
- [53] A. Melda, A. Azade, E. Fatih, C. M. C. and I. Ibrahim, "GREEN SYNTHESIS OF COPPER OXIDE NANOPARTICLES USING *OCIMUM BASILICUM* EXTRACT AND THEIR ANTIBACTERIAL ACTIVITY," *Fresenius Environmental Bulletin*, vol. 26, no. 12A, pp. 7832-7837, 2017.
- [54] A. Zahrah, "Green synthesis of copper oxide nanoparticles CuO NPs from *Eucalyptus Globoulus* leaf extract: Adsorption and design of experiments," *Arabian Journal of Chemistry*, vol. 15, 2022.
- [55] D. Henam Sylvia and S. Thiyam David, "Synthesis of Copper Oxide Nanoparticles by a Novel Method and its Application in the Degradation of Methyl Orange," *Advance in Electronic and Electric Engineering*, vol. 4, no. 1, pp. 83-88, 2014.
- [56] M. Alaa El Din, A. Khairia M., A. Sahab O., A. Salma F. and F. A. Alsamhan, "Green copper oxide nanoparticles for lead, nickel, and cadmium removal from contaminated water," *Scientific Reports*, 2021.
- [57] H. Karim H., J. Arrej A. and S. Sally K., "Synthesis of Copper Oxide Nanoparticle as an Adsorbent for Removal of Cd (II) and Ni (II) Ions from Binary System," *International Journal of Applied Environmental Sciences*, vol. 12, no. 11, pp. 1841-1861, 2017.
- [58] T. Meron Moges, C. Garima, K. Manish, P. S.P., F. Molla and Y. Priya, "Green Synthesis of Copper-oxide Nanoparticles and Evaluation of Its Therapeutic Efficacy," *Macromol. Symp.*, vol. 407, pp. 1-7, 2023.
- [59] K. Obakeng P., A. Adeyemi O., E. Saheed E. and F. Omolola E., "Green and Traditional Synthesis of Copper Oxide Nanoparticles—Comparative Study," *nanomaterials*, vol. 10,

- no. 2502, pp. 1-19, 2020.
- [60] S. I., "Green synthesis of metal nanoparticles using plants," *Journal of Green Chemistry*, vol. 13, pp. 2638-2650, 2011.
- [61] M. A., H. A. and A. M. A., "Synthesis characterization, and antimicrobial activity of copper oxide nanoparticles," *Journal of Nanomaterials*, p. 4, 2014.
- [62] D. D., B. C. Nath, P. P. and D. S. K., "Synthesis and evaluation of antioxidant and antibacterial behavior of CuO nanoparticles," *Colloids and Surfaces B: Biointerfaces*, vol. 101, pp. 430-433, 2019.
- [63] X. J., L. Z., X. P., X. L. and Y. Z., "Nanosized copper oxide induces apoptosis through oxidative stress in podocytes," *Archives of Toxicology*, vol. 87, no. 6, pp. 1067-1073, 2013.
- [64] F. B. and C. S. A., "Copper oxide nanoparticles induce oxidative stress and cytotoxicity in airway epithelial cells," *Toxicology in Vitro*, vol. 23, no. 7, pp. 1365-1371, 2009.
- [65] M. B. M. B., R. B. K. and S. T., "Bioavailability and Crop Uptake of Trace Elements in Soil Columns Amended with Sewage Sludge Products," *Plant and Soil*, vol. 262, no. 1-2, pp. 71-84, 2004.
- [66] W. D. A., "A technique for Measurement of Lead Tolerance in Plants," *Nature*, vol. 180, no. 4575, pp. 37-38, 1957.
- [67] K. K. Yadav, "Mechanistic understanding and holistic approach of phytoremediation: a review on application and future prospects," *Ecol. Eng.*, vol. 120, pp. 274-298, 2018.